Study on Moc3 as a Transcription Activator of RNAi-dependent Heterochromatin Establishment

RNAi 依存的ヘテロクロマチン形成における

転写活性化因子としての Moc3 に関する研究

Laboratory of Bioorganic Chemistry,
Graduate School of Chemical Sciences and Engineering,
Hokkaido University

Miyuki Mori

2024

Table of Contents

Abstract 3

1. Introduction 4

1-1. Centromere and Pericentromere

1-2. Heterochromatin

1-3. RNAi dependent heterochromatin formation in *S. pombe*

1-4. Bi-directional transcription of pericentromere

1-5. Moc3

1-6. Purpose of this study

2. Experimental procedure 13

2-1. Strains and media

2-2. Silencing assay

2-3. Mini-chromosome stability assay

2-4. RT-qPCR

2-5. ChIP-qPCR

2-6. Yeast one-hybrid assay

2-7. siRNA analysis

2-8. Clr4 reintroduction

2-9. Conversion rate of colony color

2-10. Chronological life span (CLS) measurement

Table 2. Strains used in this study

Table 3. Primers used in this study

Table 4. Antibodies used in this study

3. Results 21

3-1. Identification of moc3+ as a potential positive regulator of pericentromeric ncRNA transcription.

3-2. Moc3 is not required for the maintenance of pericentromeric heterochromatin.

3-3. Moc3 assists *dh-Fw* transcription when heterochromatin integrity is impaired.
3-4. Moc3 localizes to pericentromeric heterochromatin through its zinc finger domain.
3-5. Moc3 contributes to the efficient establishment of pericentromeric heterochromatin.
3-6. Moc3 prolongs the chronological life span of cells in the stationary phase by suppressing heterochromatin over-accumulation in rDNA repeats.

4. Discussion 39
4-1. Regulation of *dh*-transcription during the establishment and maintenance of heterochromatin.
4-2. Moc3 affects the establishment of heterochromatin not only in *dh* but also in *dg*.
4-3. Moc3 is involved in facultative heterochromatin.
4-4. Functional homologs of Moc3 in other eukaryotes.

5. Conclusions 43

6. References 44

7. Acknowledgements 51

Abstract

Transcription from pericentromeric heterochromatin and its transcripts have crucial roles in diverse cellular processes such as heterochromatin establishment, heterochromatin maintenance, genome stability, and early embryo development. In higher eukaryotes, the misregulation of transcription from heterochromatin results in cancers and other harmful diseases. In fission yeast *Schizosaccharomyces pombe*, heterochromatin is established and maintained primarily by RNA interference (RNAi) dependent system. A core process of RNAi-dependent heterochromatin formation is widely conserved in various eukaryotes; the production of small interfering RNA (siRNA) and the targeting of siRNA-bound Argonaute to chromatin using its sequence complementarity. In addition, transcription from heterochromatin by RNA polymerase II is critical for providing substrates for siRNA synthesis and a platform for assembling RNAi factors. However, the detailed mechanism of transcriptional regulation and the transcription factors are still unclear. To date, various heterochromatin factors have been identified by genetic screening using fission yeast. Here, we attempted to find novel genes whose products are involved in the transcriptional regulation of pericentromeric heterochromatin by reverse genetic screening. In the screening, we found that a zinc finger protein Moc3 localizes pericentromeric heterochromatin through its zinc finger domain. It activates strand-specific transcription when heterochromatin structure or heterochromatin-dependent silencing is compromised. Although Moc3 is not essential for heterochromatin maintenance, the absence of Moc3 significantly reduces the efficient establishment of heterochromatin. These results indicate that Moc3 acts as a transcriptional activator of pericentromeric heterochromatin to induce RNAi-dependent heterochromatin establishment.

1. Introduction

1-1. Centromere and Pericentromere

Centromeres and their flanking pericentromeres are crucial chromosomal loci that ensure proper chromosome segregation at each cell division. In mitosis, the attachment of spindle microtubules to the centromere and the cohesion between sister chromatids is essential for faithful segregation, and the lack of them leads to aneuploidy and cancer. Based on the dependency of underlying DNA sequence, there are two types of centromeres: point centromeres and regional centromeres. The budding yeast has point centromeres which contain short consensus sequences to recruit centromeric DNA-binding proteins. Eukaryotic cells, including human, mouse, fly, and fission yeast, have regional centromeres containing highly repetitive sequences called satellite DNA that are epigenetically inherited throughout generations [1].

Eukaryotic genomes are packaged into a nucleus by folding its chromatin structure. Chromatin is composed of nucleosomes with a basic unit of DNA packaging, whose DNA is wrapped around an octamer of core histone proteins H2A, H2B, H3, and H4 and appears as beads on string structure (Figure 1A). Chromatin plays a key role in multiple cellular processes such as gene transcription, DNA repair, and replication by its structural dynamics which is regulated by posttranslational modifications [2]. The chromatin structure itself acts defensively against biological reactions that use genomic DNA as a substrate, but further positive and negative regulation can be triggered depending on post-translational modifications to histone proteins, making the analysis of ambivalent chromatin regulation mechanisms so difficult.

Histones have non-allelic isoforms, called histone variants, which substitute core histone proteins in nucleosomes and alter nucleosome stability and higher-order chromatin structure. Histone variants play diverse roles in cell division, transcriptional regulation, DNA repair, epigenetic inheritance, and genome stability [3]. At the site of kinetochore formation, the centromere-specific nucleosomes are constituted by the histone H3 variant CENP-A (centromere protein A), which defines centromere as an epigenetic mark. CENP-A is loaded by CENP-A specific histone chaperone at the centromere nucleosome, and non-coding RNA (ncRNA) transcription promotes its incorporation [4]. On the other hand, at pericentromere, higher-order chromatin structures of heterochromatin are formed and maintain genome stability. The formation and maintenance of heterochromatin is also regulated by the transcription of ncRNA [5]. A recent study revealed that histone H2A variant H2A.Z maintains the heterochromatin integrity by

suppressing ncRNA transcription [6]. Thereby the transcription of ncRNAs is an important process for both centromere and pericentromere.

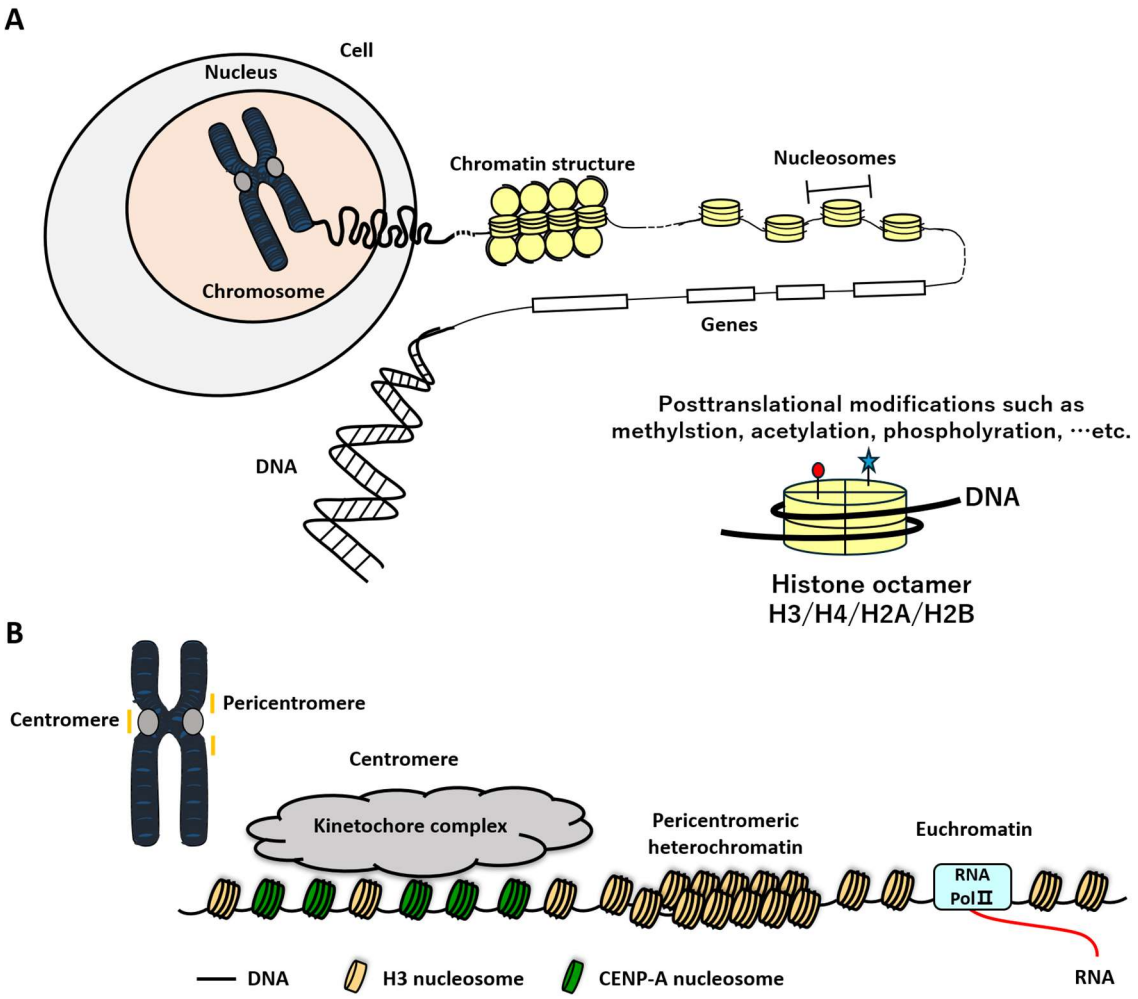

Figure 1. Chromatin structure

(A) Eukaryotic genomes are packaged into a nucleus by folding chromatin. Chromatin is composed of nucleosomes with a basic unit of DNA packaging, whose DNA is wrapped around an octamer of core histone proteins H2A, H2B, H3, and H4 and appears as beads on string structure.

(B) Two types of chromatin structure: heterochromatin and euchromatin. Euchromatin is a less condensed, open chromatin structure and is found in gene-rich transcriptionally active regions. Heterochromatin is a less accessible, condensed chromatin structure and is found in transcriptionally repressed regions. At the site of kinetochore formation, the centromere-specific nucleosomes are constituted by the histone

H3 variant CENP-A (centromere protein A) which defines centromere as an epigenetic mark. On the other hand, at pericentromere, higher-order chromatin structures of heterochromatin are formed and maintain genome stability.

1-2. Heterochromatin

Based on the structural and functional features, chromatin is categorized into euchromatin and heterochromatin (Figure 1B). Euchromatin is a less condensed, open chromatin structure found in gene-rich transcriptionally active regions. Acetylation of histone tail in euchromatin reduces the affinity between histones and DNA, facilitating active transcription. On the other hand, heterochromatin is a less accessible, condensed chromatin structure found in transcriptionally repressed regions where histones are hypoacetylated. Methylation of histone H3 at lysin 9 (H3K9me) and binding of Heterochromatin protein 1 (HP1) to H3K9me is an epigenetic mark of heterochromatin. Condensation of HP1 exhibits liquid-liquid phase separation (LLPS) properties in vitro, which may result in heterochromatin forming a membrane-less liquid-like compartment in the nucleus [7].

Heterochromatin is divided into two subcategories: facultative heterochromatin and constitutive heterochromatin. Facultative heterochromatin is usually present at developmentally regulated loci, where the chromatin can switch transcriptionally active and inactive states in response to developmental, differentiation, and environmental signals. In response to environmental signals such as nutrient conditions, temperature, and DNA damaging agents, facultative heterochromatin scattered throughout genomes are assembled and disassembled to regulate gene expression for cell survival [12, 35, 36]. Constitutive heterochromatin is present at certain genomic loci, such as pericentromeric regions, sub-telomeric regions, and transposable elements in every cell type, and once established, stably propagated through cell division [5].

1-3. RNAi dependent heterochromatin formation in *S. pombe*

The fission yeast *Schizosaccharomyces pombe* is one of the ideal model organisms for studying heterochromatin since it has more simple but also fundamental mechanisms for assembling heterochromatin compared to higher eukaryotes. In *S. pombe*, heterochromatin assembly is regulated by DNA-dependent and RNA-dependent multiple pathways. In the DNA-dependent pathway, DNA-binding proteins bind to specific DNA sequences and recruit histone modifiers to

form heterochromatin [5-7]. On the other hand, in RNA-dependent pathways, RNA interference (RNAi) machinery or RNA elimination machinery processes transcripts produced from heterochromatic regions, and then recruits histone modifiers and other heterochromatin proteins [8-14]. Heterochromatin is assembled through multiple processes: nucleation, spreading, and maintenance. In the initial process, heterochromatin is formed at the site of nucleation by RNAi, then the heterochromatin structure spreads to the surrounding region, and the heterochromatin region is maintained stably by several mechanisms (Figure 2).

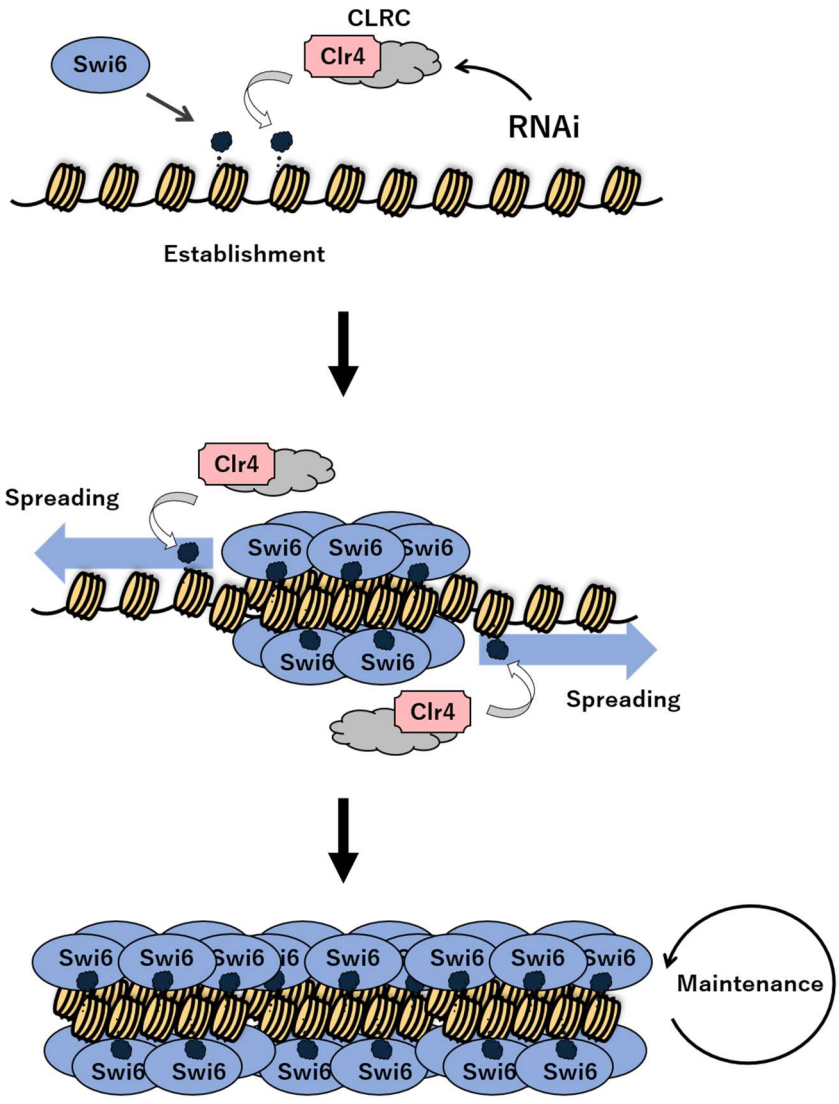

Figure 2. Process of heterochromatin formation

Schematic diagram of heterochromatin formation. For details, see text.

The centromere consists of distinct DNA elements: central core (*cnt*), innermost repeat (*imr*), and outer repeat (*otr*) [20]. Kinetochore complex is assembled on *cnt* and parts of the *imr* region, while heterochromatin is assembled on *otr* (subdivided into *dg* and *dh* repeat sequences) and parts of the *imr* region (Figure 3A). The assembly of pericentromeric heterochromatin mainly depends on the RNAi pathway, which is the mechanism of post-transcriptional gene silencing (PTGS). In the RNAi pathway, ncRNA is transcribed by RNA Polymerase II (PolII) and processed into small interfering RNAs (siRNA) [16-18]. siRNAs derived from *dg*/*dh* repeats are loaded into Argonaute protein Ago1, a component of RNA-induced transcriptional silencing (RITS) [24]. RITS targets chromatin by using sequence complementarity between siRNA and nascent ncRNA, followed by recruits RNA-dependent RNA polymerase complex (RDRC) containing Rdp1 to synthesize double-stranded RNA (dsRNA) [20, 21]. dsRNA is processed into siRNAs by Dicer ribonuclease Dcr1, thereby amplifying siRNA production. RITS also recruits the CLRC complex containing Clr4, a sole histone H3K9 methyltransferase of *S. pombe* and a homolog of mammalian Suv39h [22, 23]. The methylated H3K9 by Clr4 is recognized by chromodomain (CD) of the mammalian HP1 homolog Swi6 and Chp2 to form heterochromatin [24-26]. In addition, the Facilitates chromatin transcription (FACT) complex promotes the formation of higher-order heterochromatin structures by regulating histone turnover [32]. The binding of other chromodomain (CD) proteins, Clr4, and Chp1, which is a component of RITS, to H3K9me facilitates further recruitment of RNAi factors and histone modifiers on heterochromatin. Thereby, siRNA production and heterochromatin formation enhance each other, forming a feedback loop (Figure 3B).

HP1 proteins also contain chromo-shadow domain (CSD), which is important for their dimerization and interaction with various factors such as Clr3 and Epe1. Clr3 is a histone deacetylase (HDAC) and a component of the Snf2/HDAC repressor complex (SHREC) [33]. Clr3 and other HDACs deacetylate histones and maintain high concentrations of H3K9me in pericentromere, thereby promoting heterochromatin spreading [28, 29]. A jmjC-domain protein Epe1 is recruited to pericentromere by Swi6 to activate ncRNA transcription from the widespread transcription start site of *dg*/*dh* and promote RNAi-dependent heterochromatin formation [30, 31]. The accumulation of heterochromatin proteins at the nucleation site reinforces the formation and spreading of heterochromatin, thereby establishing heterochromatin-mediated transcriptional gene silencing (TGS).

In eukaryotes, the expression of satellite DNA is strictly regulated under physiological conditions, and environmental stress, such as heat shock, DNA damaging agents, and hyperosmotic stress, results in the upregulation of heterochromatin transcription [53, 54]. In *S. pombe*, facultative heterochromatin is assembled at meiotic genes, genes regulated by growth

conditions, retrotransposons, and rDNA repeats. In mitotic cells, meiotic mRNA is degraded by Mmi1-mediated exosome and MTREC (Mtl1-Red1 core), which is the RNA processing and surveillance complex, facilitating RNAi-independent assembly of facultative heterochromatin termed as heterochromatin islands [13, 14, 55]. In response to nutritional signals, heterochromatin islands are disassembled and induce sexual differentiation [38]. Cells grown at low glucose, low temperature, or in the absence of exosome Rrp6, facultative heterochromatin termed as heterochromatin domains (HOODs) are observed at meiotic genes, genes encoding transmembrane proteins, and retrotransposons. HOODs are regulated by RNAi, MTREC, and CCR4-NOT complex [14, 57, 58, 59].

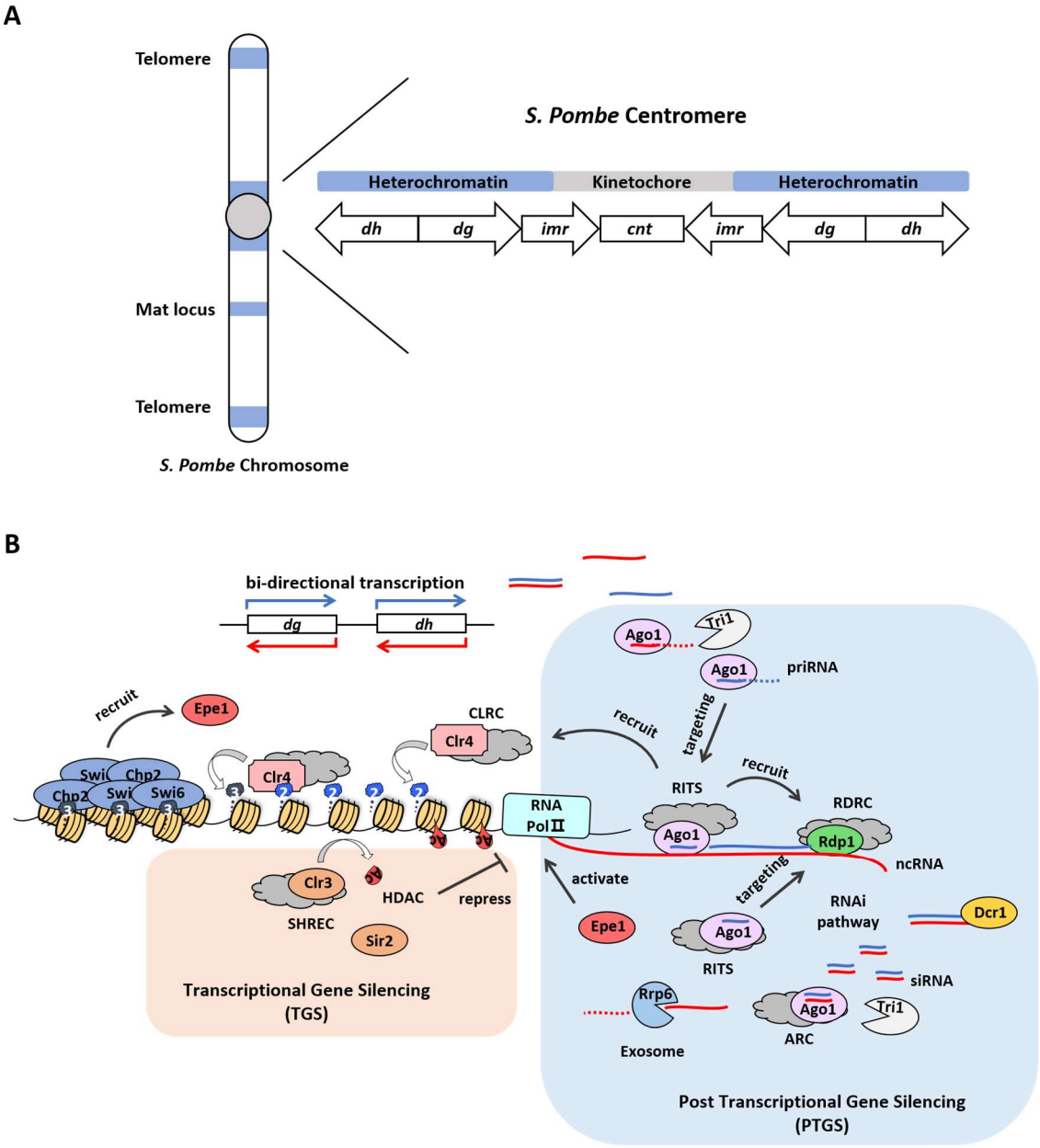

Figure 3. *S. pombe* centromere and RNAi-dependent heterochromatin formation

(A) *S. pombe* centromere consists of distinct DNA elements: central core (*cnt*), innermost repeat (*imr*), and outer repeat (*otr*). Kinetochore complex is assembled on *cnt* and parts of the *imr* region, while heterochromatin is assembled on *otr* (subdivided into *dg* and *dh* repeat sequences) and parts of the *imr* region.

(B) Schematic diagram of RNAi-dependent heterochromatin formation. For details, see text.

1-4. Bi-directional transcription of pericentromere

Previous studies revealed that *dg*/*dh* repeat sequences of pericentromeric heterochromatin are transcribed both in the forward and reverse strands. Forward transcripts are increased in *swi6*, *dcr1*, and PolII mutant cells, which disrupts heterochromatin, indicating that forward transcripts may be primarily silenced by TGS. On the other hand, reverse transcripts are also increased in *dcr1* and *swi6* mutant cells, but decreased in PolII mutant cells, indicating that reverse transcripts may be primarily silenced by PTGS [8, 17]. Transcription of *dg/dh* is activated by Epe1, an epigenetic activator associated with Swi6, but it is speculated that other regulatory factors, such as classical DNA-binding transcription factors, may also regulate transcription from *dg/dh*.

In *S.pombe*, Dicer-independent small RNA termed primal small RNA (priRNA) triggers the de novo assembly of heterochromatin. As a transcriptome surveillance mechanism, Ago1 catches degradation products of forward and reverse transcripts resulting from bi-directional transcription of pericentromeric *dg*/*dh* repeats. Ago1-associated RNA is trimmed by 3'-5'exonuclease Triman (Tri1) to generate a mature length of small RNA, then induces RNAi machinery and initiates heterochromatin formation. Tri1 is required for efficient establishment but not maintenance of heterochromatin [38, 39]. The efficient production of siRNA at the nucleation site is important for heterochromatin assembly, and dsRNA resulting from bi-directional transcription also provides a siRNA source by being the substrate for Dcr1 (Figure 3B). However, detailed mechanisms and roles of strand-specific transcription and its transcriptional regulators are still unknown.

1-5. Moc3

In *S. pombe*, sexual differentiation is induced by nutrient starvation and is downregulated by cAMP. In the cAMP pathway, under nutrient-rich conditions, a putative glucose receptor transmembrane protein Git3 activates trimeric G proteins Gpa2/Git5/Git11, releasing the α-subunit of Gpa2 to activate adenylate cyclase Cyr1. Cyr1 catalyzes the production of cAMP from ATP, and a high concentration of cAMP dissociates the regulatory subunit of Protein Kinase A, Cgs1, from the catalytic subunit, Pka1. Pka1 translocates to the nucleus and inactivates the zinc-finger transcription factor Rst2 through phosphorylation, and Rst2 represses the transcription of *ste11*, which is the main transcription factor responsible for the initiation of sexual differentiation [40].

The zinc finger protein Moc3 which has a zinc finger (Zn (2)-Cys (6)) motif, is identified as a multicopy suppressor of overexpressed Cyr1 (Moc), and the deletion of *moc3+* induces sexual differentiation even in the presence of elevated levels of cAMP. The *moc3Δ* cells are sensitive to $CaCl_2$ and DNA damaging agents such as methyl methanesulfonate (MMS) and UV, indicating that Moc3 is involved in cell survival against stress, maintaining DNA integrity and damage control [41]. However, the detailed function and roles of Moc3 remain unclear.

1-6. Purpose of this study

In this study, we tried to find new genes involved in the transcription from pericentromeric heterochromatin. We searched the *S. pombe* database to narrow down the factor and found that disruption of Moc3 reduced *dh-Forward* transcripts. Moc3 specifically localized at pericentromeric *dh* repeat sequences in a zinc finger-dependent manner, and overexpression of *moc3+* significantly activated the transcription from *dh-Fw*. Furthermore, the absence of Moc3 resulted in the reduction of efficient heterochromatin establishment. Therefore, we propose that Moc3 is required for the efficient establishment of RNAi-dependent constitutive heterochromatin via activating the transcription from *dh* repeats.

2. Experimental procedure

2-1. Strains and media

The *S. pombe* strains used in this study are listed in Table 2. The yeast media were prepared concerning PombeNet Forsburg Lab (https://dornsife.usc.edu/pombenet/media/) and genetic procedures were previously described [42]. Yeast cells were cultured in YES at 30 °C. Deletion of *moc3+* and epitope tagging were performed by PCR-based methods. For overexpression of Moc3, *moc3-5FLAG::Kan Mx* or *moc3ΔZn-5FLAG::Kan Mx* fragment was inserted into the *urg1+* locus by replacing it with *urg1+* ORF. Fragment insertion and protein levels were confirmed by colony PCR and western blotting, respectively.

2-2. Silencing assay

The silencing assay was performed as described previously [43] with the following modifications: Cells in the logarithmic growth phase were harvested and suspended in 6.25% glycerol to a concentration of 2×10^7 cells/mL. A 10-fold dilution series of cells were spotted on the following indicator plates: N/S (YES), YES without adenine (Low Ade), YES containing 5-fluoroorotic acid (0.1% 5-FOA), and YES containing TBZ (15 μg/mL TBZ). The plates were then incubated at 30 °C for 3 – 4 days.

2-3. Mini-chromosome stability assay

The mini-chromosome stability assay was performed as described previously [44] with the following modifications: Using Ch16 mini-chromosome carrying cells [45], Ade+ white colonies on YE plates were cultivated in YE at 30 °C. Cells in the logarithmic growth phase were harvested and suspended in sterile water to a concentration of 2×10^4 cells/mL. 1000 cells were plated on YE plates to measure *I* (the initial percentage of cells carrying the mini-chromosomes). 10000 cells from the same cultures were cultivated in YES at 30 °C for 10 – 15 generations, after which cells were harvested and suspended in sterile water to a concentration of 2×10^4 cells/mL. 1000 cells were plated on YE plates to measure *F* (the final percentage of cells carrying the mini-chromosomes). The mini-chromosome loss rate per division was calculated from the following formula: loss rate $=[1-(F/I)^{1/N}]*100$. *N* is the number of generations between *I* and *F*.

2-4. RT-qPCR

RT-PCR was performed as described previously [46]. Briefly, total RNA was isolated from 1×10^8 cells in the logarithmic growth phase using the hot phenol method and then treated with

Recombinant DNase I (RNase-free) (Takara Bio). Using gene-specific primers, 1 μg of total RNA was reverse transcribed into cDNA with PrimeScript Reverse Transcriptase (Takara Bio). Gene-specific primers are listed in Table 3. qPCR was performed after RT-PCR. PCR mixtures containing SYBR dye were used to run the Thermal Cycler Dice Real-Time System (Takara Bio). Primers used for qPCR are listed in Table 3.

2-5. ChIP-qPCR

ChIP assay was performed as described previously [47] with the following modifications: Reverse crosslinking was performed by adding 1/50 volume of 5 M NaCl and incubating at 95 °C for 20 minutes. DNA was then purified by phenol/chloroform extraction and ethanol precipitation. The antibodies used for immunoprecipitation are listed in Table 4. Only Moc3 ChIP (anti-FLAG) was immunoprecipitated for 3 hours and others were 2 hours. qPCR was performed after the ChIP assay. PCR mixtures containing SYBR dye were used to run the Thermal Cycler Dice Real-Time System (Takara Bio). Primers used for qPCR are listed in Table 3.

2-6. Yeast one-hybrid assay

Yeast one-hybrid assay was performed as described previously [48]. Strains carrying reporter plasmid [SP463 (GAL10 UAS-mel1) or SP466 (dh UAS-mel1)] were transformed with activator expression plasmids [SP476 (Moc3ZF::pREP1), SP470 (Moc3ZF-Gal4AD::pREP1), SP468 (Gal4DB-Gal4AD::pREP1) and SP469 (Gal4DB-VP16c::pREP1)]. Transformants were spotted on EMM media containing 40ng/μl X-alpha-Gal and incubated at 30 °C for 4-8 days.

2-7. siRNA analysis

Detection of siRNA was performed as described previously [49]. Briefly, small RNA was isolated from 1×10^9 cells in the logarithmic growth phase using the mirVana miRNA Isolation Kit (Ambion). 15 μg of small RNA was separated on 15% polyacrylamide/7 M urea gel and then transferred to Hybond N + nylon transfer membrane (GE Healthcare). DNA oligonucleotide probes corresponding to siRNA sequences derived from *dg* and *dh* repeats [50] or snoRNA69 were labeled with [γ -^{32}P] ATP and then hybridized to the membrane using ULTRAhyb-Oligo buffer (Ambion). DNA oligos are listed in Table 3.

2-8. Clr4-ON/OFF experiment

Yeast strains were cultivated on PMG 5S + 2 μM Thiamine plates at 30 °C. Cells were cultured in PMG 5S + 2 μM Thiamine liquid medium, and cells in the logarithmic growth phase were washed by sterile water three times, suspended in PMG 5S medium (- Thiamine) to a concentration of 2.5×10^5 cells/mL, and cultured at 30 °C for 10 days. ChIP and RT-PCR samples

were collected on the day0 before transfer to - Thiamine medium and on the day5 after transfer, respectively.

2-9. Conversion rate of colony color

Using *moc3Δ clr4+ (re)* cells, a single pink or red colony on the YE plate was suspended in sterile water to a concentration of 2×10^4 cells/mL. 1000 cells were plated on a YE plate to measure *I* (the initial percentage of pink or red cells). 10000 cells from the same suspension were cultivated in YES at 30 °C for 13 – 17 generations, after which cells were harvested and suspended in sterile water to a concentration of 2×10^4 cells/ml. 1000 cells were plated on a YE plate to measure *F* (the final percentage of pink or red cells). The conversion rate of colony color per 10 generations was calculated from the following formula: Conversion rate = $[1-(F/I)^{10/N}]\times100$. N is the number of generations between *I* and *F*.

2-10. Chronological life span (CLS) measurement

L972 strain was grown on the YES plate at 30 °C and a single colony was grown on the YES-liquid medium. The next day, the number of cells was measured, and the culture medium was diluted with sterile water and spread on YES plates. After 4 days, the number of colonies was counted (number of colonies = number of living cells). The higher number of colonies on the next day and the day after the start of culture was counted as day 0 (100% survival, no more division), and the cells were plated on consecutive days to follow their lifespan over time.

Table 1. Genes analyzed in this study

Systematic ID	Name	TBZ *1	Description
SPAC23D3.09	*arp42*	S	SWI/SNF and RSC complex subunit Arp42
SPBC13G1.08c	*ash2*	S	Ash2-trithorax family protein, Set1 complex, Lid2 complex
SPCC736.08	*cbf11*	S	CBF1/Su(H)/LAG-1 family transcription factor Cbf11
SPAC1782.09c	*clp1*	S	Cdc14-related protein phosphatase Clp1/Flp1
SPAC4D7.07c	*csi2*	S	mitotic chromosome segregation protein Csi2
SPCC1223.10c	*eaf1*	-	RNA polymerase II transcription elongation factor SpEAF
SPBP23A10.14c	*ell1*	-	RNA polymerase II transcription elongation factor SpELL
SPCC1393.08	*fil1*	S	transcription factor, zf-GATA type (predicted)
SPAC1952.05	*gcn5*	S	SAGA complex histone acetyltransferase catalytic subunit Gcn5
SPAC26H5.05	*mga2*	S	IPT/TIG ankyrin repeat gene-specific transcription coactivator Mga2
SPAC821.07c	*moc3*	R	transcription factor Moc3
SPBC651.09c	*prf1*	S	RNA polymerase II-associated Paf1 complex (predicted)
SPBC2F12.11c	*rep2*	S	transcriptional activator, MBF subunit Rep2
SPAC18B11.07c	*rhp6*	S	Rad6 homolog, ubiquitin-conjugating enzyme E2 Rhp6
SPCC306.04c	*set1*	S	histone lysine methyltransferase Set1
SPCC594.05c	*spf1*	S	Set1C PHD Finger protein Spf1, Set1 complex
SPBC354.03	*swd3*	S	WD repeat protein Swd3, Set1 complex
SPBC1539.02 *2		-	conserved eukaryotic nuclear protein implicated in meiotic chromosome segregation

*1. S and R mean sensitivity to TBZ. respectively, which is reported in Pombase (www.pombase.org)

*2. The amino acid sequence of the *SPBC1539.02* gene has a high homology compared to that of the *dot1* gene (*S. cerevisiae* H3K79 methyl transferase).

Table 2. Strains used in this study

Name	Genotype	Source
FY336	*h-, ade6-m210, leu1-32, ura4-DS/E, cnt1/TM(NcoI)::ura4+*	R. Allshire
HKV292	*h-, ade6-m210, leu1-32, ura4-DS/E, cnt1/TM(NcoI)::ura4+, clr4Δ::Kan Mx*	Our stock
M78	*h- (L972 strain)*	Our stock
M167	*h-, ade6-m210, leu1-32, ura4-DS/E, cnt1/TM(NcoI)::ura4+,arp42Δ::Hph Mx*	This study
M122	*h-, ade6-m210, leu1-32, ura4-DS/E, cnt1/TM(NcoI)::ura4+, ash2Δ::Hph Mx*	This study
M125	*h-, ade6-m210, leu1-32, ura4-DS/E, cnt1/TM(NcoI)::ura4+, cbf11Δ::Hph Mx*	This study
M128	*h-, ade6-m210, leu1-32, ura4-DS/E, cnt1/TM(NcoI)::ura4+, clp1Δ::Hph Mx*	This study
M119	*h-, ade6-m210, leu1-32, ura4-DS/E, cnt1/TM(NcoI)::ura4+, csi2Δ::Hph Mx*	This study
M131	*h-, ade6-m210, leu1-32, ura4-DS/E, cnt1/TM(NcoI)::ura4+, eaf1Δ::Hph Mx*	This study
M134	*h-, ade6-m210, leu1-32, ura4-DS/E, cnt1/TM(NcoI)::ura4+, ell1Δ::Hph Mx*	This study
M358	*h-, ade6-m210, leu1-32, ura4-DS/E, cnt1/TM(NcoI)::ura4+, fil1Δ::Hph Mx*	This study

M137	*h-, ade6-m210, leu1-32, ura4-DS/E, cnt1/TM(NcoI)::ura4+, gcn5Δ::Hph Mx*	This study
M203	*h-, ade6-m210, leu1-32, ura4-DS/E, cnt1/TM(NcoI)::ura4+,mga2Δ::Hph Mx*	This study
M367	*h-, ade6-m210, leu1-32, ura4-DS/E, cnt1/TM(NcoI)::ura4+, moc3Δ::Hph Mx*	This study
M218	*h-, ade6-m210, leu1-32, ura4-DS/E, cnt1/TM(NcoI)::ura4+, prfΔ::Hph Mx*	This study
M206	*h-, ade6-m210, leu1-32, ura4-DS/E, cnt1/TM(NcoI)::ura4+,rep2Δ::Hph Mx*	This study
M174	*h-, ade6-m210, leu1-32, ura4-DS/E, cnt1/TM(NcoI)::ura4+,rhp6Δ::Kan Mx*	This study
M215	*h-, ade6-m210, leu1-32, ura4-DS/E, cnt1/TM(NcoI)::ura4+, set1Δ::Hph Mx*	This study
M140	*h-, ade6-m210, leu1-32, ura4-DS/E, cnt1/TM(NcoI)::ura4+, spf1Δ::Hph Mx*	This study
M143	*h-, ade6-m210, leu1-32, ura4-DS/E, cnt1/TM(NcoI)::ura4+, swd3Δ::Hph Mx*	This study
M116	*h-, ade6-m210, leu1-32, ura4-DS/E, cnt1/TM(NcoI)::ura4+, SPBC1539.02Δ::Hph Mx*	This study
FY2002	*h+, ade6-DN/N, leu1-32, ura4-DS/E, imr1L::ura4+, otr1R::ade6+*	R. Allshire
M379	*h+, ade6-DN/N, leu1-32, ura4-DS/E, imr1L::ura4+, otr1R::ade6+, moc3Δ::Hph Mx*	This study
M472	*h+, ade6-DN/N, leu1-32, ura4-DS/E, imr1L::ura4+, otr1R::ade6+, moc3Δ::Nat Mx*	This study
SFY30	*h+, ade6-DN/N, leu1-32, ura4-DS/E, imr1L::ura4+, otr1R::ade6+, clr4Δ::Nat Mx*	Our stock
M389	*h+, ade6-DN/N, leu1-32, ura4-DS/E, imr1L::ura4+, otr1R::ade6+, clr4Δ::Nat Mx, moc3Δ::Hph Mx*	This study
KKS-141	*h+, ade6-DN/N, leu1-32, ura4-DS/E, imr1L::ura4+, otr1R::ade6+, clr3Δ::Hph Mx*	Our stock
M506	*h+, ade6-DN/N, leu1-32, ura4-DS/E, imr1L::ura4+, otr1R::ade6+, clr3Δ::Hph Mx, moc3Δ::Nat Mx*	This study
KKS-358	*h+, ade6-DN/N, leu1-32, ura4-DS/E, imr1L::ura4+, otr1R::ade6+, rdp1Δ::Hph Mx*	Our stock
M509	*h+, ade6-DN/N, leu1-32, ura4-DS/E, imr1L::ura4+, otr1R::ade6+, rdp1Δ::Hph Mx, moc3Δ::Nat Mx*	This study
FY520	*h+, ade6-m210, leu1-32, ura4-DS/E, ch16m23(ade6-m216)-ura4+-TEL*	R. Allshire
HKV300	*h+, ade6-m210, leu1-32, ura4-DS/E, ch16m23(ade6-m216)-ura4+-TEL, clr4Δ::Kan Mx*	Our stock
M249	*h+, ade6-m210, leu1-32, ura4-DS/E, ch16m23(ade6-m216)-ura4+-TEL, arp42Δ::Hph Mx*	This study
M197	*h+, ade6-m210, leu1-32, ura4-DS/E, ch16m23(ade6-m216)-ura4+-TEL, ash2Δ::Hph Mx*	This study
M191	*h+, ade6-m210, leu1-32, ura4-DS/E, ch16m23(ade6-m216)-ura4+-TEL, cbf11Δ::Hph Mx*	This study
M183	*h+, ade6-m210, leu1-32, ura4-DS/E, ch16m23(ade6-m216)-ura4+-TEL, clp1Δ::Hph Mx*	This study
M180	*h+, ade6-m210, leu1-32, ura4-DS/E, ch16m23(ade6-m216)-ura4+-TEL, csi2Δ::Hph Mx*	This study
M237	*h+, ade6-m210, leu1-32, ura4-DS/E, ch16m23(ade6-m216)-ura4+-TEL, eaf1Δ::Hph Mx*	This study
M246	*h+, ade6-m210, leu1-32, ura4-DS/E, ch16m23(ade6-m216)-ura4+-TEL, ell1Δ::Hph Mx*	This study
M296	*h+, ade6-m210, leu1-32, ura4-DS/E, ch16m23(ade6-m216)-ura4+-TEL, fil1Δ::Hph Mx*	This study
M240	*h+, ade6-m210, leu1-32, ura4-DS/E, ch16m23(ade6-m216)-ura4+-TEL, gcn5Δ::Hph Mx*	This study
M194	*h+, ade6-m210, leu1-32, ura4-DS/E, ch16m23(ade6-m216)-ura4+-TEL, mga2Δ::Hph Mx*	This study
M300	*h+, ade6-m210, leu1-32, ura4-DS/E, ch16m23(ade6-m216)-ura4+-TEL, moc3Δ::Hph Mx*	This study
M242	*h+, ade6-m210, leu1-32, ura4-DS/E, ch16m23(ade6-m216)-ura4+-TEL, prf1Δ::Hph Mx*	This study
M186	*h+, ade6-m210, leu1-32, ura4-DS/E, ch16m23(ade6-m216)-ura4+-TEL, rep2Δ::Hph Mx*	This study
M243	*h+, ade6-m210, leu1-32, ura4-DS/E, ch16m23(ade6-m216)-ura4+-TEL, rhp6Δ::Kan Mx*	This study
M190	*h+, ade6-m210, leu1-32, ura4-DS/E, ch16m23(ade6-m216)-ura4+-TEL, set1Δ::Hph Mx*	This study
M200	*h+, ade6-m210, leu1-32, ura4-DS/E, ch16m23(ade6-m216)-ura4+-TEL, spf1Δ::Hph Mx*	This study
M189	*h+, ade6-m210, leu1-32, ura4-DS/E, ch16m23(ade6-m216)-ura4+-TEL, swd3Δ::Hph Mx*	This study

M177	*h+, ade6-m210, leu1-32, ura4-DS/E, ch16m23(ade6-m216)-ura4+-TEL, SPBC1539.02Δ::Hph Mx*	This study
TKY1031	*h90, ura4-DS/E, leu1-32, ade6-DN/N, chp1-mycx6-his3, his3-D1?,kint2::ura4+, otr1R::ade6+*	Our stock
TKY1174	*h90, ura4-DS/E, leu1-32, ade6-DN/N, chp1-mycx6-his3, his3-D1?, kint2::ura4+, otr1R::ade6+, clr4Δ::Nat Mx*	Our stock
TKY3534	*h90, ura4-DS/E, leu1-32, ade6-DN/N, chp1-mycx6-his3, his3-D1?, kint2::ura4+, otr1R::ade6+, clr4Δ::Nat Mx, clr4-hph-pTP(Re)*	Our stock
TKY3549	*h90, ura4-DS/E, leu1-32, ade6-DN/N, chp1-mycx6-his3, his3-D1?, kint2::ura4+, otr1R::ade6+, dcr1Δ::Kan Mx, clr4Δ::Nat Mx, clr4-hph-pTP(Re)*	Our stock
M405	*h-, moc3 Δ::Hph Mx*	
M534	*h90, ura4-DS/E, leu1-32, ade6-DN/N, chp1-mycx6-his3, his3-D1?, kint2::ura4+, otr1R::ade6+, moc3Δ::Hph Mx*	This study
M548	*h90, ura4-DS/E, leu1-32, ade6-DN/N, chp1-mycx6-his3, his3-D1?, kint2::ura4+, otr1R::ade6+, moc3Δ::Nat Mx, clr4Δ::Kan Mx*	This study
M551	*h90, ura4-DS/E, leu1-32, ade6-DN/N, chp1-mycx6-his3, his3-D1?, kint2::ura4+, otr1R::ade6+, moc3Δ::Nat Mx, clr4Δ::Kan Mx, clr4-hph-pTP(Re)_pink#1*	This study
M553	*h90, ura4-DS/E, leu1-32, ade6-DN/N, chp1-mycx6-his3, his3-D1?, kint2::ura4+, otr1R::ade6+, moc3Δ::Nat Mx, clr4Δ::Kan Mx, clr4-hph-pTP(Re)_red#1*	This study
M580	*h90, ura4-DS/E, leu1-32, ade6-DN/N, chp1-mycx6-his3, his3-D1?, kint2::ura4+, otr1R::ade6+, moc3Δ::Nat Mx, clr4Δ::Kan Mx, clr4-hph-pTP(Re)_pink#2*	This study
M582	*h90, ura4-DS/E, leu1-32, ade6-DN/N, chp1-mycx6-his3, his3-D1?, kint2::ura4+, otr1R::ade6+, moc3Δ::Nat Mx, clr4Δ::Kan Mx, clr4-hph-pTP(Re)_red#2*	This study
AHT506	*h+, ade6-DN/N, leu1-32, otr1R::ade6+, ura4-D18, clr4Δ::P81nmt1-3FLAG-clr4-spo5 DSR*	Our stock
M961	*h+, ade6-DN/N, leu1-32, otr1R::ade6+, ura4-D18, clr4Δ::P81nmt1-3FLAG-clr4-spo5 DSR, moc3Δ::Hph Mx*	This study
M973	*h+, ade6-DN/N, leu1-32, otr1R::ade6+, ura4-D18, clr4Δ::P81nmt1-3FLAG-clr4-spo5 DSR, dcr1Δ::Hph Mx*	This study
SFY830	*h+, ade6-M216, his2, leu1, ura4*	Our stock
M633	*h+, ade6-DN/N, leu1-32, ura4-DS/E, imr1L::ura4+, otr1R::ade6+, moc3-5FLAG::Kan Mx*	This study
M686	*h+, ade6-DN/N, leu1-32, ura4-DS/E, imr1L::ura4+, otr1R::ade6+, moc3Δ::Hph Mx , urg1::moc3-5FLAG::Kan Mx*	This study
M760	*h+, ade6-DN/N, leu1-32, ura4-DS/E, imr1L::ura4+, otr1R::ade6+, moc3-5FLAG::Kan Mx, clr4Δ::Nat Mx*	This study
M783	*h+, ade6-DN/N, leu1-32, ura4-DS/E, imr1L::ura4+, otr1R::ade6+, moc3-5FLAG::Kan Mx, clr3Δ::Hph Mx*	This study
M811	*h+, ade6-DN/N, leu1-32, ura4-DS/E, imr1L::ura4+, otr1R::ade6+, moc3Δ::Nat Mx , urg1::moc3-5FLAG::Kan Mx, clr3Δ::Hph Mx*	This study
M905	*h+, ade6-DN/N, leu1-32, ura4-DS/E, imr1L::ura4+, otr1R::ade6+, moc3Δ::Nat Mx , urg1::moc3ΔZn-5FLAG::Kan Mx*	This study
M911	*h+, ade6-DN/N, leu1-32, ura4-DS/E, imr1L::ura4+, otr1R::ade6+, moc3Δ::Nat Mx , urg1::moc3ΔZn-5FLAG::Kan Mx, clr3Δ::Hph Mx*	This study
M792	*h+, ade6-DN/N, leu1-32, ura4-DS/E, imr1L::ura4+, otr1R::ade6+, moc3-5FLAG::Kan Mx, dcr1Δ::Hph Mx*	This study
M795	*h+, ade6-DN/N, leu1-32, ura4-DS/E, imr1L::ura4+, otr1R::ade6+, moc3Δ::Nat Mx , urg1::moc3-5FLAG::Kan Mx, dcr1Δ::Hph Mx*	This study
M849	*h+, ade6-DN/N, leu1-32, ura4-DS/E, imr1L::ura4+, otr1R::ade6+, moc3-5FLAG::Kan Mx, rdp1Δ::Hph Mx*	This study
M852	*h+, ade6-DN/N, leu1-32, ura4-DS/E, imr1L::ura4+, otr1R::ade6+, moc3Δ::Nat Mx , urg1::moc3-5FLAG::Kan Mx, rdp1Δ::Hph Mx*	This study

Table 3. Primers used in this study

Name	Sequence	Used for
SF75/pFA6a Fw	CGGATCCCCGGGTTAATTAA	Amplification of marker cassette
SF76/pFA6a Rv	GAATTCGAGCTCGTTTAAAC	Amplification of marker cassette
mf255/moc3Δ Rv	TTAATTAACCCGGGGATCCGAACTGCAAGGGAAACAATAGATAG	*moc3*+ deletion
mf256/moc3Δ Fw	GTTTAAACGAGCTCGAATTCTTTTAAAATCATTTTGATGCTTTTC	*moc3*+ deletion
mf266/moc3ΔZn Rv	CATGGCTTGCATTTGAGCAGCTCTTTTTGTGGGCTTGGGC	*moc3*+ zinc finger deletion
mf267/moc3ΔZn Fw	GCCCAAGCCCACAAAAAGAGCTGCTCAAATGCAAGCCATG	*moc3*+ zinc finger deletion
EOO-141/act1 Fw	TGCCGATCGTATGCAAAAGG	RT-PCR
EOO-142/act1 Rv	CCGCTCTCATCATACTCTTG	RT-PCR
EOO-474/imr Fw	GCGTGAATATTGATGTTTTGAG	ChIP
EOO-475/imr Rv	ATACTAGTGATGCAAGCGTTC	ChIP
EOO-532/dh RT1 (dh_2)	CACCAGACCATTACAAGCAC	ChIP
EOO-533/dh RT2 (dh_2)	TCTCGCCTATTTACCGATCC	ChIP
EOO-544/dh_3 Fw	TCAGCAGTCCTTGGGAAATG	ChIP
EOO-545/dh_3 Rv	CTGTCAGGATGTGTTGTCGTTC	ChIP
KKO-019/adh1 Fw	CTGCCCTCACATTCAACTTTCC	ChIP, RT-PCR
KKO-624/dg_2 Fw	CTGCGGTTCACCCTTAACATC	ChIP
KKO-625/dg_2 Rv	CAACTGCGGATGGAAAAAGT	ChIP
Nakama305/dg_3 Fw	ATTACTGGAGTTCAGCCGAC	ChIP
Nakama306/dg_3 Rv	CGTGTACTAGAGCAATTCGG	ChIP
mf39/dg Fw	TCCATCCCAGCTGAACAAATAC	ChIP, RT-PCR (RT primer for dg Rv)
mf40/dg Rv	TCAACATACGCTCTCCATGTAC	ChIP, RT-PCR (RT primer for dg Fw)
mf41/imr-dg Fw	GTAGGATGGGTTTAGATGTTTTCAG	ChIP
mf42/imr-dg Rv	GGATACTATTTTGGACAGAATGGATG	ChIP
mf47/tra1 ORF Fw	CAAGCAGAAGAAGAAGAAGACAC	ChIP
mf48/tra1 ORF Rv	AGCAGACTCAATGTTAGTGGC	ChIP
mf86/adh1 Rv	CACGATAGCAAGTGATACCAGC	ChIP, RT-PCR
mf264/dh RT3 (dh)	CTCTCATCTCGACTCGTTTG	ChIP, RT-PCR
mf265/dh RT4 (dh)	GGCATTCACGAAACATAGCG	ChIP, RT-PCR (RT primer for dh Fw)
p30F	CCATATCAATTTCCCATGTTCC	RT-PCR (RT primer for dh Rv) ※1
p30R	CATCAAGCGAGTCGAGATGA	RT-PCR ※1
mf319/clr4_RT_F1	GGATGCTCAGAACTATGGAG	RT-PCR
mf320/clr4_RT_R1	AAAGCGAGATCATAAATGG	RT-PCR
18S-rDNA-5' (586)	CCTGCCAGTAGTCATATGCTTG	ChIP
18S-rDNA-3' (587)	GACTCACCAAAAAAAGCCCG	ChIP
28S-rDNA-5' (743)	CACCTGCCGAATGAACTAGC	ChIP
28S-rDNA-3' (744)	CCCAAGGCTTCGTCACAAA	ChIP

mf290/snoRNA69	CAATGTAAATACTCCGAGTGAGCTGGGTTTAAC	siRNA analysis ※2
mf291/cen dg siRNA	GCGACTAAACCGAAAGCCTC	siRNA analysis ※2
mf292/cen dg siRNA	TACCGTGATTAGCCTTACTCCGCATT	siRNA analysis ※2
mf293/cen dg siRNA	GGGAGTACATCATTCCTACTTCGATA	siRNA analysis ※2
mf294/cen dg siRNA	GACTTTCAAAGATGCACA	siRNA analysis ※2
mf295/cen dg siRNA	TTTTCTCTTTCAAAAGTA	siRNA analysis ※2
mf296/cen dg siRNA	CAATTGGAAGTACATCCA	siRNA analysis ※2
mf297/cen dg siRNA	TCAATCCATCATGTACGA	siRNA analysis ※2
mf298/cen dg siRNA	AATTCGATTCCAAGTACA	siRNA analysis ※2
mf299/cen dg siRNA	ATTGTTTCGACAACACGA	siRNA analysis ※2
mf300/cen dh siRNA	TACCGCTTCTCCTTAATCCA	siRNA analysis ※2
mf301/cen dh siRNA	ACACCTACTCTTATCACTTGT	siRNA analysis ※2
mf302/cen dh siRNA	GACGATAAGCAGGAGTTGCGCA	siRNA analysis ※2
mf303/cen dh siRNA	AGTGTGGCGCTATATCTTGTA	siRNA analysis ※2
mf304/cen dh siRNA	TACTGTCATTAGGATATGCTCA	siRNA analysis ※2
mf305/cen dh siRNA	GGGAAATGTATAAATAGGCA	siRNA analysis ※2
mf306/cen dh siRNA	TTTCCCAAGGACTGCTGAGGTAGA	siRNA analysis ※2
mf307/cen dh siRNA	TGGCAGATATTGCAAGTTGTTTA	siRNA analysis ※2
mf308/cen dh siRNA	TTTGATGCCCATGTTCATTCCACTTG	siRNA analysis ※2

※1 Kloc A, Zaratiegui M, Nora E, Martienssen R. RNA interference guides histone modification during the S phase of chromosomal replication. Curr Biol. 2008 Apr 8;18(7):490-5. doi: 10.1016/j.cub.2008.03.016.

※2 Holoch, D., Moazed, D. (2015). Small-RNA loading licenses Argonaute for assembly into a transcriptional silencing complex. Nat Struct Mol Biol, 22, 328–335. https://doi.org/10.1038/nsmb.2979

Table 4. Antibodies used in this study

Name	Source
H3K9me1/2/3 (m5.1.1)	Gifted from Professor Takeshi Urano.
CTD phosphorylated Ser2 (CMA603)	Gifted from Professor Hiroshi Kimura.
RNA polymerase II CTD (8WG16)	Abcam
RNA polymerase II CTD (4H8)	Millipore
FLAG (M2)	Sigma

3. Results

3-1. Identification of *moc3*+ as a potential positive regulator of pericentromeric ncRNA transcription.

To identify the factor that regulates transcription within the pericentromeric heterochromatin, we performed reverse genetic analysis. We focused on the sensitivity of microtubule inhibitor TBZ (thiabendazole), which is often caused by heterochromatin disruption [51]. We expected that factors with the gene deletion phenotype of TBZ-sensitivity or resistance might contain key factors that regulate heterochromatin and pick up some candidate genes from PomBase (https://www.pombase.org/), a public database for fission yeast (Figure 4). Table 1 lists the 18 candidate genes analyzed in this study that appear to regulate transcription, chromatin modification, and chromatin structure. Note that *clp1*+, a Cdc14-related protein phosphatase, was chosen as a non-chromatic protein control and *clr4*+ as a known heterochromatic gene. Since all candidate genes were non-essential, we constructed a deletion mutant and tested the altered phenotype to TBZ. Most candidate strains showed the same phenotype as reported in the database, but some strains differed: deletion of *gcn5* did not affect TBZ sensitivity, while deletion of *fil1* or *rhp6* resulted in slight resistance to TBZ (Figure 5A). We also examined the effect of candidate genes on centromere function by measuring the stability of the mini-chromosome. In wild-type cells, non-essential mini-chromosome Ch16 is replicated like other chromosomes at each cell division and is stably inherited by daughter cells, while in *clr4Δ* cells, the mini-chromosome is gradually lost at each cell division because heterochromatin is completely disrupted, and centromeres do not function properly. Indeed, in *clr4Δ* cells, the rate of mini-chromosome loss per cell division was 12.8-fold higher than in WT cells. In TBZ-sensitive cells, the loss rate was higher than in wild-type cells, but in TBZ-resistant cells, excluding *moc3Δ,* and cells without the TBZ phenotype, the loss rate was comparable to wild-type cells (Figure 5B). These results indicate that centromere dysfunction is indeed responsible for TBZ sensitivity and that cells exhibiting a TBZ phenotype, and high mini-chromosome loss rates may contain target strains.

To investigate whether these TBZ phenotypes reflect the transcriptional defect within the heterochromatin, we measured the accumulation of non-coding transcripts from the pericentromeric repeats (*dh-Fw*) by strand-specific RT-PCR (Figure 5C). Most candidates showed no change compared to wild-type cells, while some candidates, such as *arp42Δ*, *gcn5Δ,* and *rep2Δ* cells showed a slight increase (but less than four-fold). Surprisingly, only *moc3Δ* cells showed a half decrease relative to wild-type cells (P-value < 0.05), suggesting that Moc3 positively

regulates *dh-Fw* transcription (Figure 5D). This unusual phenotype of *moc3Δ* cells in *dh-Fw* transcription prompted us to further analyze.

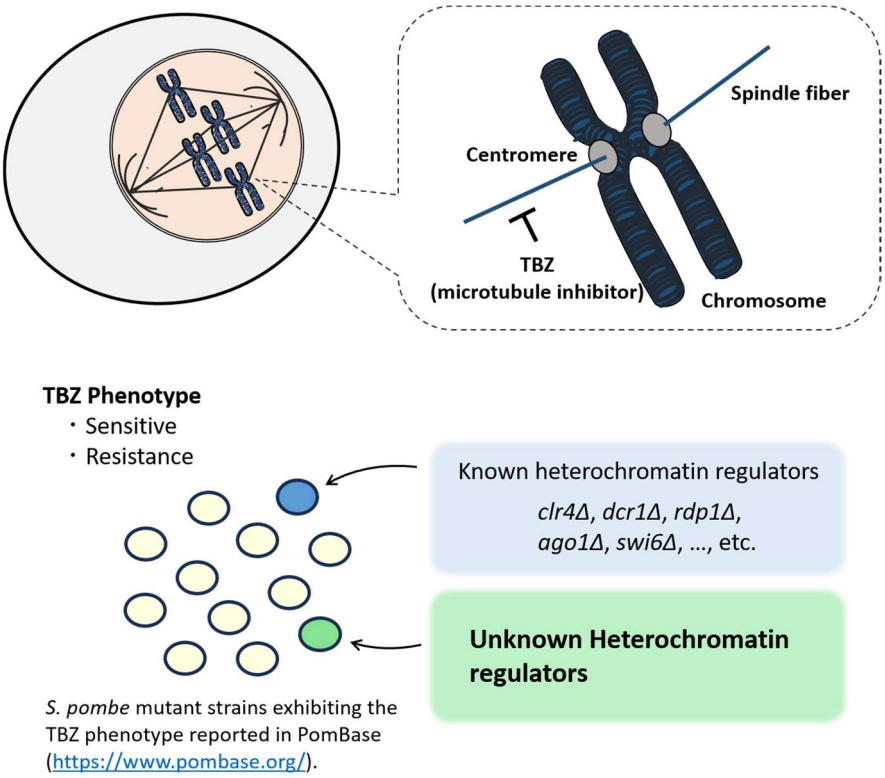

Figure 4. Overview of the screening.

The microtubule inhibitor TBZ (thiabendazole) results in severe growth defects in heterochromatin mutants. We expected that factors with the gene deletion phenotype of TBZ in PomBase (https://www.pombase.org/) might contain key factors that regulate heterochromatin.

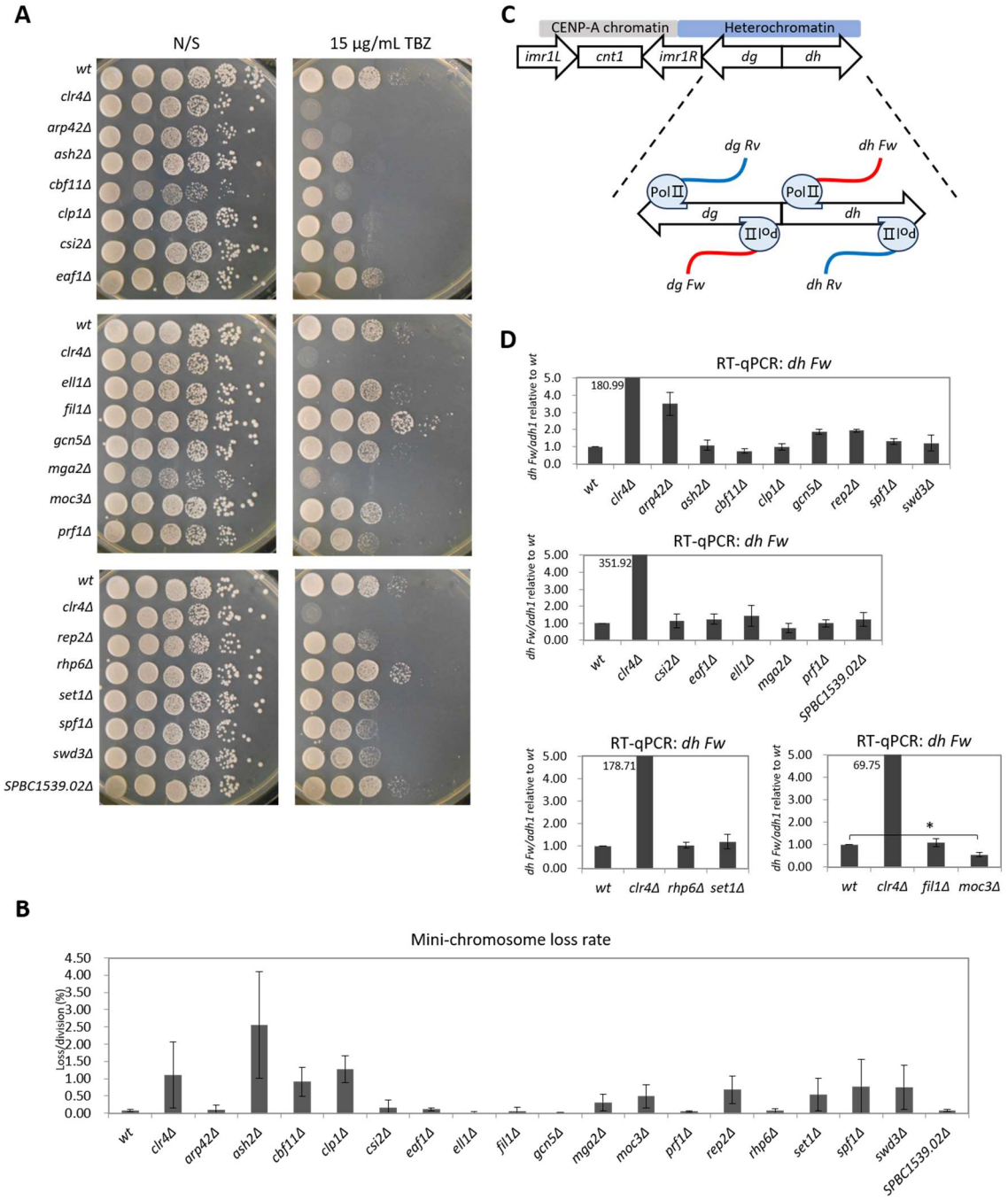

Figure 5. Identification of *moc3*+ as a transcriptional regulator of pericentromeric heterochromatin.

(A) Sensitivity to the TBZ. The ten-fold serial dilution strains were spotted on non-selective medium (YES) and YES containing thiabendazole (15 μg/mL TBZ).

(B) Mini-chromosome stability of the non-essential mini-chromosome Ch16 during cell division in indicated strains. The loss rate was calculated from the following formula: loss rate = $1-(F/I)^{1/N}$ (I; the initial percentage of cells carrying the Ch16, F; the final percentage of cells carrying the Ch16, N;

the number of generations between *I* and *F*. See EXPERIMENTAL PROCEDURE more detail). Error bars indicate the standard deviations from three independent experiments (n=3).

(C) Schematic diagram of transcriptional orientation in *dg* and *dh* repeats.

(D) Quantitative RT-PCR (RT-qPCR) of dh forward transcripts in indicated strains. Expression levels were normalized by *adh1+* and shown as a fold increase relative to wild-type. Error bars indicate the standard deviations from three independent experiments (n=3). P-value was determined using a two-sided Student's t-test: *p<0.05.

3-2. Moc3 is not required for the maintenance of pericentromeric heterochromatin.

To examine the effect of Moc3 on pericentromeric heterochromatin, we confirmed silencing phenotype using FY2002 reporter strains with *ura4+* and *ade6+* marker genes inserted into *imr1L* and *otr1R*, respectively (*imr1L::ura4+* and *otr1R::ade6+*). However, the silencing phenotype of *moc3Δ* cells was not significantly altered compared to wild-type cells (Figure 6A and 6B). To assess the chromatin state of *dg*/*dh* repeats at the molecular level, we performed a chromatin immunoprecipitation (ChIP) assay of H3K9 methylation (H3K9me1/2/3) that is the repressive epigenetic mark of heterochromatin. The level of H3K9me in *moc3Δ* cells was not reduced compared to the wild-type cells, suggesting that heterochromatin is still maintained (Figure 6C). These results indicate that Moc3 is not required for heterochromatin maintenance. Note that the level of H3K9me in *moc3Δ* cells tended to increase, though it was not statistically significant.

To determine whether the decrease in *dh-Fw* transcripts in *moc3Δ* cells was due to the reduction of transcription, we confirmed the level of RNA PolII. However, the level of RNA PolII in *moc3Δ* cells was not significantly reduced compared to wild-type cells (Figure 6D). Since heterochromatin is kept silent and excludes RNA PolII from its locus by TGS, it is difficult to observe further reduction. In addition, unlike strand-specific RT-PCR, it is difficult to detect strand-specific localization of RNA PolII in ChIP assay. To enhance the detection sensitivity of RNA PolII in ChIP assay, we introduced *moc3Δ* into *clr4Δ* cells with increased RNA PolII level at *dg*/*dh* repeats due to complete loss of heterochromatin. In *clr4Δ* cells, the levels of RNA Pol II and RNA Pol II phosphorylated at Ser2 in the C-terminal domain (CTD-Ser2p), a mark of transcription elongation, in *dh* repeats were greatly increased compared to wild-type cells. In contrast, antibodies recognizing pan PolII, including the inactive state of PolII, did not significantly decrease (Figure 6D), but the amount of CTD-Ser2p was reduced by almost half in *clr4Δ moc3Δ* cells compared to *clr4Δ* cells (Figure 6E). These results suggest that Moc3 is involved in the transcription of *dh-Fw* by RNA Pol II.

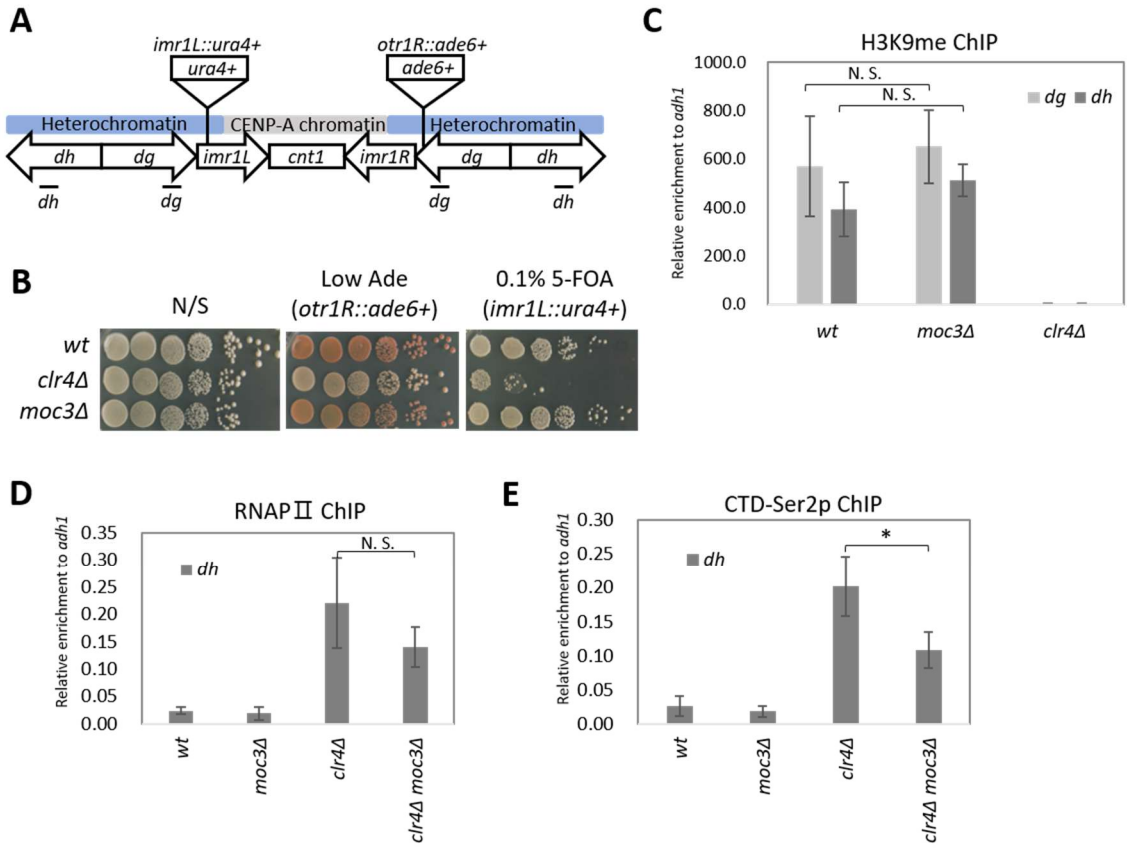

Figure 6. Moc3 is not required for the maintenance of pericentromere heterochromatin.

(A) Schematic diagram of centromere 1 region of the reporter strains used in the silencing assay. The *ade6+* and *ura4+* reporter genes were inserted into the pericentromeric region of chromosome I (*otr1R::ade6+ and imr1L::ura4+*). Black bars indicate the position of primers used in RT-PCR and ChIP assay.

(B) Silencing assay of *otr1R::ade6+ and imr1L::ura4+* reporter strain. The ten-fold serial dilution strains were spotted on a non-selective medium (YES), YES containing 5-fluoroorotic acid (0.1% 5-FOA) and YES without adenine (Low Ade) to examine the expression of a reporter gene.

(C) ChIP assay of H3K9me at dh and dg repeats or *adh1+* control locus in indicated strains. Error bars indicate the standard deviations from three independent experiments (n=3). P-value was determined using a two-sided Student's t-test: N.S. not significant.

(D, E) ChIP assay of RNAPII (D) and CTD-Ser2p (E) at *dh* repeats relative to *adh1+* control locus in indicated strains. Error bars indicate the standard deviations from three independent experiments (n=3). P-value was determined using a two-sided Student's t-test: N.S. not significant, *p<0.05.

3-3. Moc3 assists *dh-Fw* transcription when heterochromatin integrity is impaired.

To gain further insight into the heterochromatic transcription regulated by Moc3, we examined the accumulation of forward and reverse transcripts derived from *dg/dh* repeats (*dg-Fw*, *dg-Rv*, *dh-Fw*, and *dh-Rv* in Figure 7A, 7B, 7C) by RT-PCR. For the same reason as PolII ChIP, we introduced *moc3Δ* into *clr4Δ* cells to enhance the detection sensitivity of transcripts. Interestingly, in *clr4*Δ cells, the accumulation of forward transcripts generated from both *dg* and *dh* was considerably higher than that of reverse transcripts (Figure 7A). The introduction of *moc3Δ* into *clr4Δ* cells decreased the accumulation of *dh-Fw* transcripts by more than half compared to *clr4Δ* cells, while *dh-Rv*, *dg-Fw*, and *dg-Rv* transcripts did not show such a marked decrease, suggesting that Moc3 act as a positive regulator of *dh-Fw* transcription (Figure 7A).

To find additional features of Moc3 in heterochromatic transcription, we introduced *moc3Δ* into *rdp1Δ* and *clr3Δ* cells, respectively. Rdp1 is an RNAi factor and is required for dsRNA synthesis to generate siRNAs. Clr3 is a histone deacetylase and promotes heterochromatin spreading. Clr3 is a histone deacetylase (HDAC) and a component of the Snf2/HDAC repressor complex (SHREC) [30]. Clr3 and other HDACs deacetylate histones and maintain high concentrations of methylated H3K9 in pericentromere, thereby promoting heterochromatin spreading.

We examined the accumulation of transcripts by RT-PCR and found that the increase in *dh-Fw* and *dg-Fw* transcripts in both *rdp1Δ* and *clr3Δ* cells was less than 1/2 of that in *clr4Δ* cells. On the other hand, the increase in *dh-Rv* and *dg-Rv* transcripts in *clr3Δ* cells was less than 1/2 of that in *clr4Δ* cells, while the increase in *rdp1Δ* cells was comparable to that in *clr4Δ* cells (Figure 7B, 6C). These results suggest that forward transcription is regulated by multiple pathways and reverse transcription is primarily regulated by RNAi. Like the result of *clr4Δ moc3Δ* cells, *rdp1Δ moc3Δ* and *clr3Δ moc3Δ* cells also specifically reduced *dh-Fw* transcripts but not *dh-Rv*, *dg-Fw,* or *dg-Rv* compared to *rdp1Δ* and *clr3Δ* cells*,* respectively (Figure 7A, 7B, 7C). RNAPII levels in *clr3Δ moc3Δ* cells were also reduced in both *dg* and *dh* compared to *clr3Δ* cells (Figure 7D). These results indicate that Moc3 is required for efficient transcription of *dh-Fw* when heterochromatin integrity is impaired.

Since *dh-Fw* transcription is reduced in the absence of Moc3, we analyzed the effect of *moc3Δ* on *dh*-derived siRNA production. As reported previously, *dh*-derived siRNAs were increased in *clr3Δ* cells. This was because the increase in heterochromatic ncRNA in *clr3Δ* cells provides more substrate for siRNA production by RNAi [27, 29]. In *moc3Δ* cells, the level of *dh*-derived siRNA

was the same as in wild-type cells, while in *clr3Δ moc3Δ* cells, it decreased by nearly half of that in *clr3Δ* cells (Figure 7E). This result suggests that Moc3-dependent *dh-Fw* transcripts are the target of RNAi for siRNA production in *clr3Δ* cells.

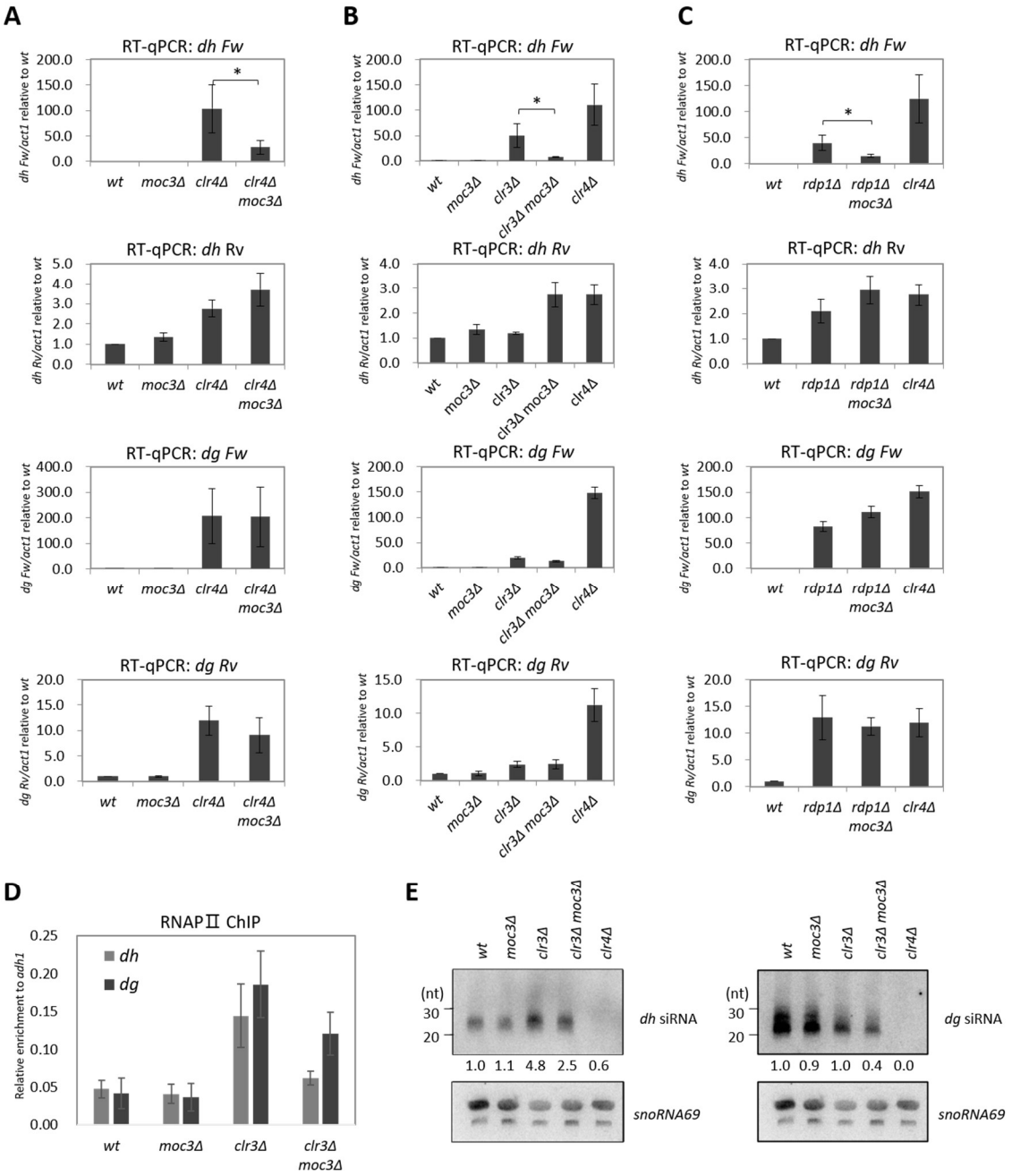

Figure 7. Moc3 specifically regulates the *dh* forward transcription.

(A-C) RT-qPCR of *dh* forward, *dh* reverse, *dg* forward, and *dg* reverse transcripts in indicated strains. Expression levels were normalized by *act1+* and shown as a fold increase relative to wild-type. Error bars indicate the standard deviations from three independent experiments (n=3). P-value was determined using a two-sided Student's t-test: *p<0.05.

(D) ChIP assay of RNAPII at *dg* and *dh* repeats relative to *adh1+* control locus in indicated strains. Error bars indicate the standard deviations from three independent experiments (n=3).

(E) Northern blots of siRNA isolated from the indicated strains. Oligonucleotide probes specific for *dh* and *dg* repeats (Holoch, & Moazed, 2015) and *snoRNA69* as a loading control were used. siRNA levels were normalized by *snoRNA69* and shown as a fold increase relative to wild-type. Biologically independent experiments were reproducible (n=2).

3-4. Moc3 localizes to pericentromeric heterochromatin through its zinc finger domain.

Since Moc3 is reported as a zinc finger domain-containing transcription factor, we expected that Moc3 binds to *dh* and activates *dh-Fw* transcription. To test this possibility, we examined the localization of Moc3-5FLAG at multiple positions in pericentromeric heterochromatin by ChIP assay with an anti-FLAG antibody (Figure 8A). In wild-type cells, no significant localization of Moc3-5FLAG at each locus was detected, whereas, in *clr4Δ* cells, significant localization of Moc3-5FLAG was observed at *dh_2,* where Moc3 contributes to *dh-Fw* transcription (Figure 8B, P-value < 0.05).

To examine the binding ability of Moc3 to the *dh_2* sequence, we performed a Yeast One Hybrid assay as reported previously [48]. In the Y1H assay, "Prey" is fused to the Gal4 activation domain (prey-Gal4 AD), and "Bait DNA sequence" is inserted into the reporter locus upstream of the *mel1+* gene. Since the *mel1+* gene is regulated by Gal4, when prey binds to bait DNA, α-galactosidase is produced, and colonies turn blue on a medium containing X-α-Gal (Figure 8C). When the zinc finger domain of Moc3 was fused as prey (Moc3 ZF-Gal4 AD) and the *dh_2* sequence was inserted as bait, the colonies on the X-α-Gal containing plate turned blue (Figure 8D). This result indicates that Moc3 binds to the *dh_2* sequence through its zinc finger domain.

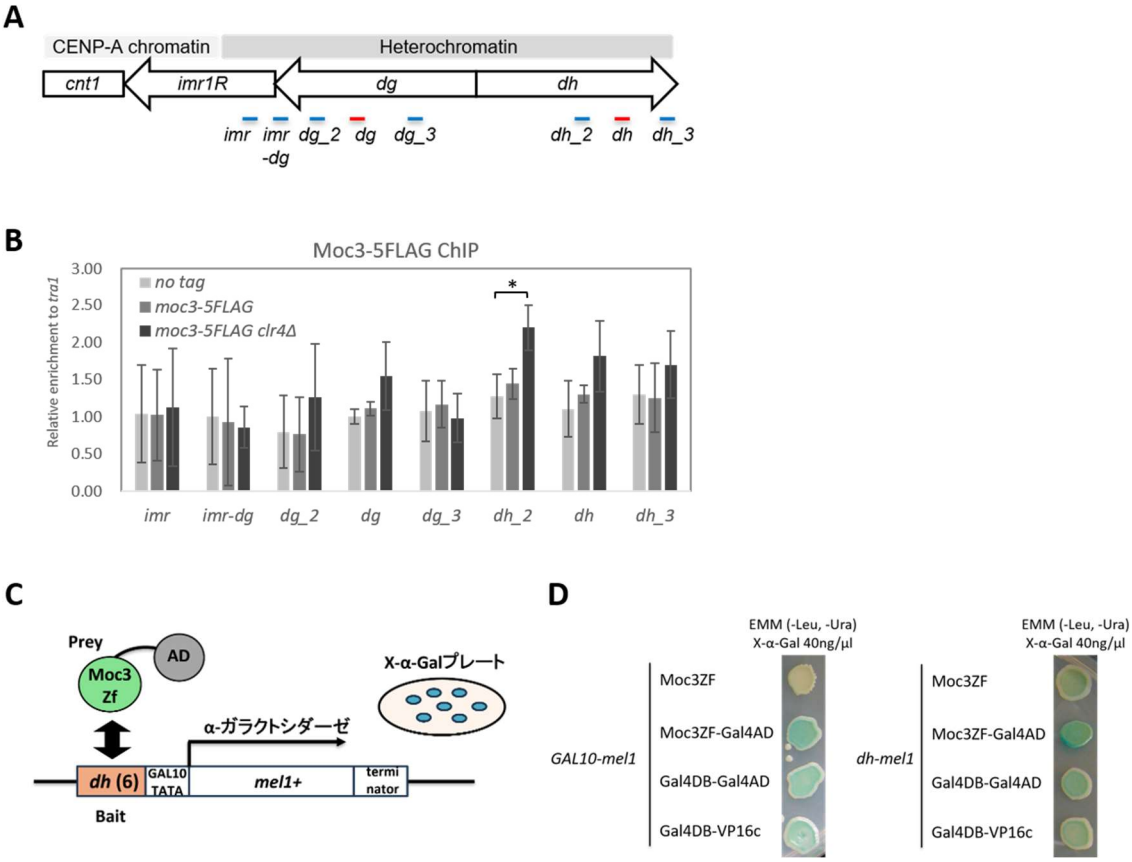

Figure 8. Moc3 binds to *dh* DNA through its zinc finger domain.

(A) Schematic diagram of centromere 1 region of the chromosome I. Blue bars indicate the position of primers used in Moc3-5FLAG ChIP. Red bars indicate the position of primers used in RT-PCR and ChIP assay.

(B) ChIP assay of Moc3-5FLAG at the indicated position described in (A) relative to *tra1*+ control locus in indicated strains. Error bars indicate the standard deviations from three independent experiments (n=3). P-value was determined using a two-sided Student's t-test: *p<0.05.

(C) Schematic diagram of the Yeast One Hybrid assay. Prey is fused to the *Gal4* activation domain (*prey-Gal4 AD*) and the bait DNA sequence is inserted into the reporter locus upstream of the *mel1*+ gene. When prey binds to the bait DNA, α-galactosidase is produced and the colonies turn blue on the medium containing X-α-Gal.

(D) Fission yeast one-hybrid assay. Strains were spotted on EMM media containing 40ng/μl X-alpha-Gal, and incubated at 30℃ for 4-8 days.

To confirm whether the zinc finger domain of Moc3 is required for *dh* binding at pericentromeric heterochromatin, we constructed a zinc finger domain truncated mutant (*moc3ΔZn-5FLAG*) and analyzed Moc3 localization by ChIP assay (Figure 9A). In wild-type cells, Moc3-5FLAG was significantly localized to *dh_2* compared to no tag cells. Furthermore, overproduction of Moc3 (*moc3-5FLAG-op*) showed more obvious localization, while deletion of the zinc finger domain (*moc3ΔZn-op*) decreased localization to the same extent as no tag cells. Importantly, the overproduction of Moc3 and Moc3ΔZn did not increase localization to *dg* (Figure 9B). These results indicate that Moc3 localized to *dh* in a zinc finger domain-dependent manner. In *clr3Δ* cells, Moc3-5FLAG localization was increased in both *dg* and *dh_2* compared to no tag cells, however, overproduction of Moc3-5FLAG tended to increase localization only in *dh_2*, although the difference was not statistically significant.

Consistent with the amount of Moc3 localization, overproduction of Moc3-5FLAG significantly increased *dh-Fw* transcripts three-fold in both wild-type and *clr3Δ* cells but did not affect *dg-Fw* transcripts. Like *moc3Δ* cells, *moc3ΔZn-op* and *moc3ΔZn-op clr3Δ* cells decreased *dh-Fw* transcripts compared to wild-type and *clr3Δ* cells, respectively (Figure 9C, 9D). These results suggest that Moc3 localizes to *dh* repeats through its zinc finger domain and regulates *dh-Fw* transcription. However, overproduction of Moc3-5FLAG or Moc3ΔZn-5FLAG in wild-type and *clr3*Δ cells did not affect the H3K9me level at *dh* (Figure 9E), probably because an adequate amount of siRNA was supplied by Epe1-dependent transcription.

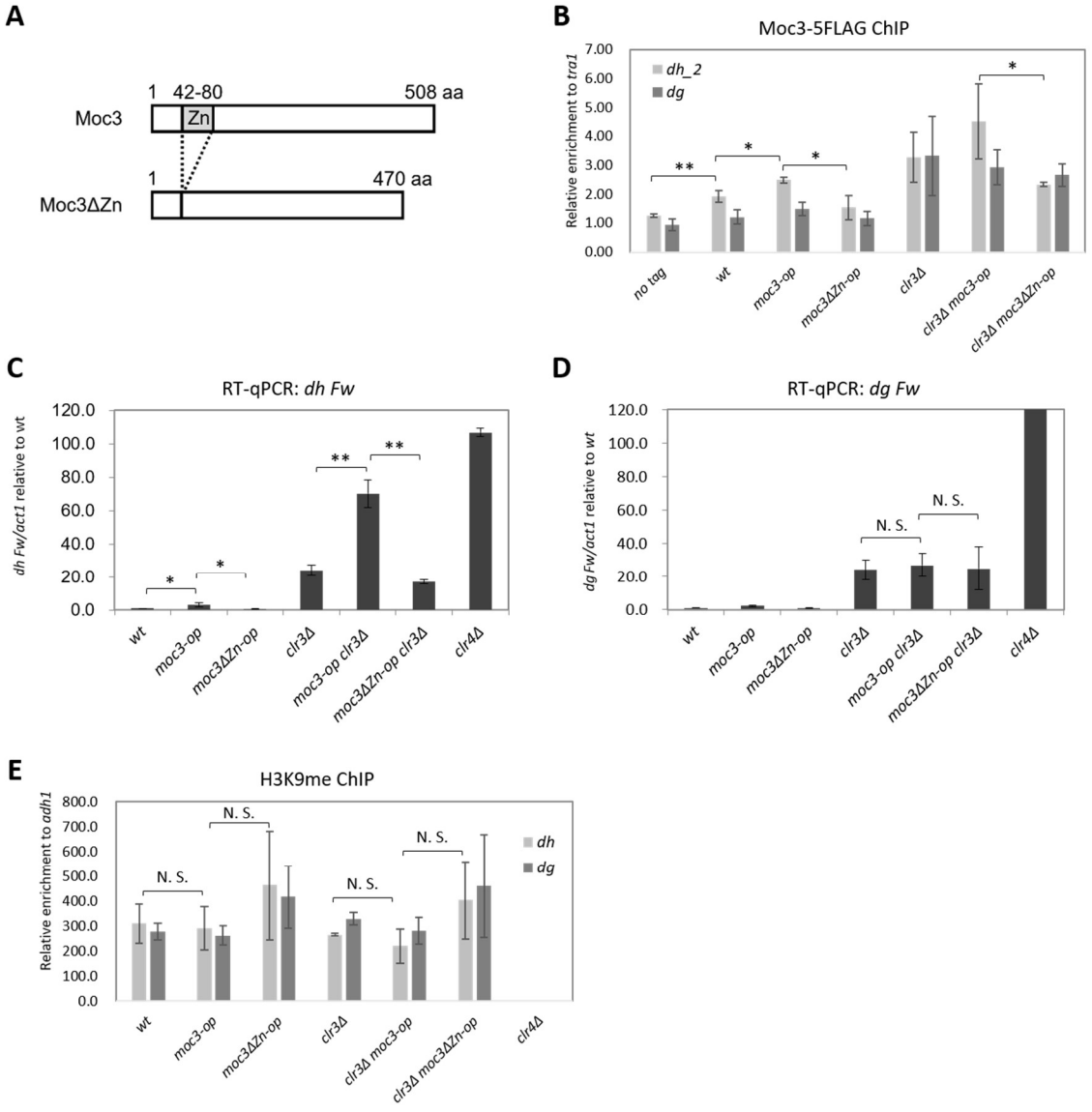

Figure 9. Moc3 activates *dh* forward transcription in a zinc finger-dependent manner.

(A) Schematic diagram of the zinc finger domain truncated Moc3 protein used in this study. The zinc finger domain is indicated by a gray box.

(B) ChIP assay of Moc3ΔZn -5FLAG at *dh_2* relative to *tra1+* control locus in indicated strains. Error bars indicate the standard deviations from three independent experiments (n=3). P-value was determined using a two-sided Student's t-test: N.S. not significant, *p<0.05, **p<0.001.

(C, D) RT-qPCR of *dh-Fw* and *dg-Fw* transcripts in indicated strains. Expression levels were normalized by *act1+* and shown as a fold increase relative to wild-type. Error bars indicate the standard deviations from three independent experiments (n=3). P-value was determined using a two-sided

Student's t-test: N.S. not significant, *p<0.05, **p<0.001.

(E) ChIP assay of H3K9me at dh and dg repeats relative to *adh1+* control locus in indicated strains. Error bars indicate the standard deviations from three independent experiments (n=3). P-value was determined using a two-sided Student's t-test: N.S. not significant.

3-5. Moc3 contributes to the efficient establishment of pericentromeric heterochromatin.

The above results indicate that Moc3 localizes to *dh* repeats and activates *dh-Fw* transcription, and resulting transcripts are the targets for RNAi. These results are observed especially when heterochromatin is compromised. This raised the possibility that Moc3 may function when heterochromatin is compromised, for example, in the initial step of the heterochromatin establishment (Figure 2). To investigate this, we performed "Clr4 add-back experiments" and monitored the effect of Moc3 on the initial step of heterochromatin establishment (Figure 10A). In this assay, we deleted the *clr4+* gene in wild-type and *moc3*Δ cells to erase all heterochromatin, then reintroduced the *clr4+* gene into the genome by electroporation and observed whether heterochromatin was re-established. To monitor the silencing states, these strains have the *ade6+* reporter gene inserted in pericentromeric heterochromatin, and in wild-type cells, repression of the *ade6+* gene results in red colonies on low adenine plate (*otr::ade6+* in Figure 6A). On the other hand, in *clr4*Δ cells, de-repression of the *ade6+* gene by erasing heterochromatin results in pink colonies on a low adenine plate. Deletion of *clr4+* also resulted in severe sensitivity to TBZ, high expression of *dh-Fw* RNA, and loss of H3K9me in *dg/dh*, which represent defects in pericentromeric heterochromatin formation (Figur10, 10C, 10E). When the *clr4+* gene was re-introduced into *clr4*Δ cells (*clr4+(re)* strain), all transformants formed red colonies on a low adenine plate and were resistant to 5-FOA, suggesting that the marker genes were silenced. Consistent with this, in *clr4+(re)* cells, *dh-Fw* transcripts were not detected and the level of H3K9me was restored to the same level as in wild-type cells (Figure 10C, 10E). These results indicate that heterochromatin was re-established and transcription from *dg/dh* was silenced in *clr4+(re)* cells. Note that the expression levels of *clr4+* in the *clr4*-transformants were significantly higher than those in the original strains (*wt* and *moc3*Δ in Figure 10D) for an unknown reason. In contrast, *moc3Δclr4+(re)* cells formed pink and red colonies on a low adenine plate. FOA and TBZ sensitivities of red clones of *moc3*Δ*clr4+(re)* were comparable to those of *clr4+(re)* cells, while pink clones were more sensitive to FOA and TBZ than red clones (Figure 10B). Although the level of *clr4+* expression in *moc3Δ clr4+ (re) pink* clones was the same as in *moc3Δ clr4+ (re) red* clones, the silencing of *dh-Fw* and the level of H3K9me were impaired at

the same level as in *moc3Δ clr4Δ* cells, suggesting that heterochromatin establishment was compromised in pink clones and the marker genes were not silenced (Figure 10C, 10E). Note that the level of H3K9me at *dg*, where Moc3 does not localize, was also low in pink colonies. These results indicate that Moc3 contributes to establishing heterochromatin at both *dg* and *dh*.

Since the pink clones of *moc3Δ clr4+ (re)* cells appeared to gradually recover TBZ and FOA sensitivity (Figure 10B), we measured the frequency of pink clones that did not re-establish heterochromatin was converted to red colonies by re-establishing heterochromatin after long-term culture. In *dcr1Δ clr4+ (re)* cells, a single pink colony did not convert to red colonies after 10 generations due to the loss of effective siRNA production and the resulting impairment of heterochromatin re-establishment. In contrast, in *moc3Δ clr4+ (re) pink* clones, a single pink colony converted to red colonies, indicating that heterochromatin was re-established. However, the frequency was very low, about 0.63-0.72% per 10 generations (Figure 10F). This result suggests that Moc3 is not essential for heterochromatin establishment, but is necessary for efficient establishment.

The stability of re-established heterochromatin was also measured by the conversion rate from single red colonies to pink colonies after long-term culture. In *clr4+ (re)* cells, a single red colony hardly converted to pink colonies after 10 generations, indicating that heterochromatin is maintained stably. In *moc3Δ clr4+ (re) red* clones, the conversion rate was comparable to that in *clr4+ (re)* cells, suggesting that once heterochromatin was re-established in *moc3Δ clr4+ (re)* cells, it is maintained stably throughout cell division (Figure 10F). This result was consistent with the results that Moc3 is not required for heterochromatin maintenance (Figure 6).

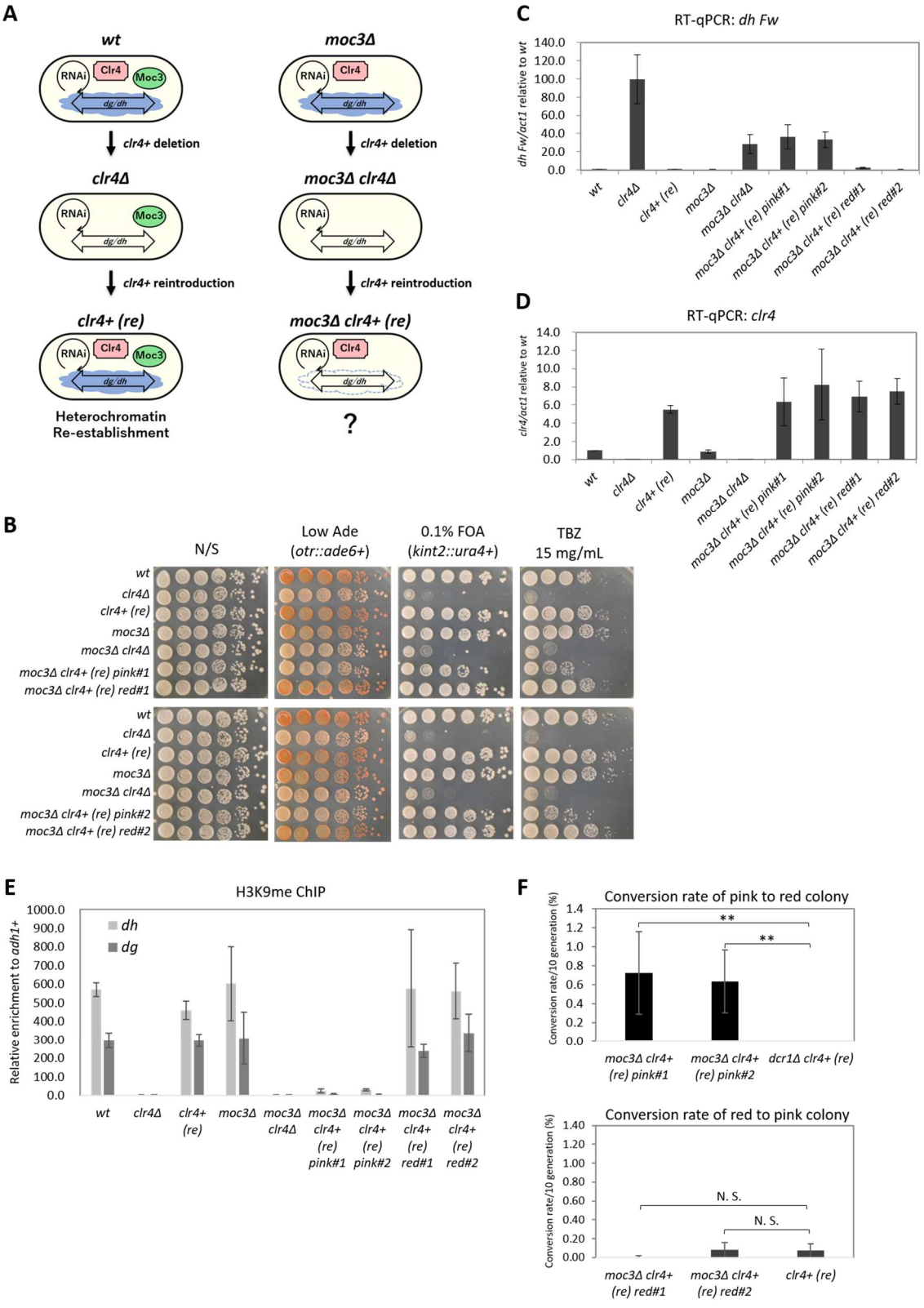
A
wt
moc3Δ
RNAi
Clr4
Moc3
dg/dh
clr4+ deletion
clr4Δ
moc3Δ clr4Δ
clr4+ reintroduction
clr4+ (re)
moc3Δ clr4+ (re)
Heterochromatin
Re-establishment
?
C
RT-qPCR: dh Fw
dh Fw/act1 relative to wt
140.0
120.0
100.0
80.0
60.0
40.0
20.0
0.0
wt
clr4Δ
clr4+ (re)
moc3Δ
moc3Δ clr4Δ
moc3Δ clr4+ (re) pink#1
moc3Δ clr4+ (re) pink#2
moc3Δ clr4+ (re) red#1
moc3Δ clr4+ (re) red#2
D
RT-qPCR: clr4
clr4/act1 relative to wt
14.0
12.0
10.0
8.0
6.0
4.0
2.0
0.0
B
N/S
Low Ade
(otr::ade6+)
0.1% FOA
(kint2::ura4+)
TBZ
15 mg/mL
wt
clr4Δ
clr4+ (re)
moc3Δ
moc3Δ clr4Δ
moc3Δ clr4+ (re) pink#1
moc3Δ clr4+ (re) red#1
moc3Δ clr4+ (re) pink#2
moc3Δ clr4+ (re) red#2
E
H3K9me ChIP
Relative enrichment to adh1+
1000.0
900.0
800.0
700.0
600.0
500.0
400.0
300.0
200.0
100.0
0.0
dh
dg
wt
clr4Δ
clr4+ (re)
moc3Δ
moc3Δ clr4Δ
moc3Δ clr4+ (re) pink#1
moc3Δ clr4+ (re) pink#2
moc3Δ clr4+ (re) red#1
moc3Δ clr4+ (re) red#2
F
Conversion rate of pink to red colony
Conversion rate/10 generation (%)
1.4
1.2
1.0
0.8
0.6
0.4
0.2
0.0
**
**
moc3Δ clr4+ (re) pink#1
moc3Δ clr4+ (re) pink#2
dcr1Δ clr4+ (re)
Conversion rate of red to pink colony
Conversion rate/10 generation (%)
1.40
1.20
1.00
0.80
0.60
0.40
0.20
0.00
N. S.
N. S.
moc3Δ clr4+ (re) red#1
moc3Δ clr4+ (re) red#2
clr4+ (re)

Figure 10. Moc3 contributes to the efficient establishment of pericentromeric heterochromatin.

(A) Schematic diagram of Clr4 add-back experiment.

(B) Silencing assay of *otr1R::ade6+* and *kint2::ura4+* reporter strain. The ten-fold serial dilution strains were spotted on non-selective medium (YES), YES without adenine (Low Ade), YES containing 5-FOA (0.1% 5-FOA), and YES containing TBZ (15 μg/mL TBZ) to examine the expression of the reporter gene.

(C, D) RT-qPCR of *dh-Fw* and *clr4+* transcripts in indicated strains. Expression levels were normalized by *act1+* and shown as a fold increase relative to wild-type. Error bars indicate the standard deviations from three independent experiments (n=3).

(E) ChIP assay of H3K9me at *dg* and *dh* repeats relative to *adh1+* control locus in indicated strains. Error bars indicate the standard deviations from three independent experiments (n=3).

(F) Conversion rate of colony per 10 generations in indicated strains. The conversion rate was calculated from the following formula: Conversion rate $=[1-(F/I)^{10/N}]*100$ (*I*; the initial percentage of the pink or red colonies, *F*; the final percentage of the pink or red colonies, N; the number of generations between *I* and *F*. See EXPERIMENTAL PROCEDURE more detail). Error bars indicate the standard deviations from three independent experiments (n=3). P-value was determined using a two-sided Student's t-test: N.S. not significant, **p<0.001.

To further investigate, we developed a system to monitor the heterochromatin re-establishment using a strain in which *clr4+* expression can be controlled. In this system, the *clr4+* gene was expressed from the *nmt1-81* promoter, which has mutations in the core promoter sequence of the original *nmt1* promoter, resulting in low levels of basal and induced transcription in response to thiamine removal from the medium [52]. To further eliminate the trace expression of *clr4+* under the repressive condition, we fused the 3' end of the *clr4+* coding sequence with a determinant of selective removal sequence (DSR) derived from *mei4+* (*nmt1-81-clr4-DSR* in Figure 11A). DSR is recognized by an RNA-binding protein Mmi1 during mitotic cell growth and degraded by an exosome-dependent RNA elimination machinery [53]. Instead of the *clr4+* gene, we introduced the *nmt1-81-clr4-DSR* into wild-type, *moc3*Δ, and *dcr1*Δ cells. In a medium containing thiamine, *clr4+* RNA is degraded by Mmi1 mediated exosome, and *clr4+* expression is turned off, whereas, in a medium without thiamine, *clr4+* expression is induced and turned on (Figure 11A). In cells before the removal of thiamine from the medium, degradation of *clr4+* RNA resulted in the loss of H3K9me levels in *dg/dh*, indicating that heterochromatin was erased (Day 0 in Figure 11B, 11C). After transferring cells to a thiamin-free medium, *clr4+* expression was induced at the same level in wild-type, *moc3Δ*, and *dcr1Δ* cells (Day 5 in Figure 11B, 11C). In wild-type cells,

expression of *clr4*+ RNA restored high levels of H3K9me accumulation in *dg/dh*, while in *dcr1Δ* cells, the accumulation of H3K9me was prevented, confirming that RNAi is essential for the establishment of heterochromatin (Figure 11C). In agreement with the results of the Clr4 add-back experiment, the deletion of *moc3*+ could not fully restore the levels of H3K9me in *dg/dh* compared to wild-type cells. These results support the idea that Moc3 is involved in *de novo* formation of heterochromatin.

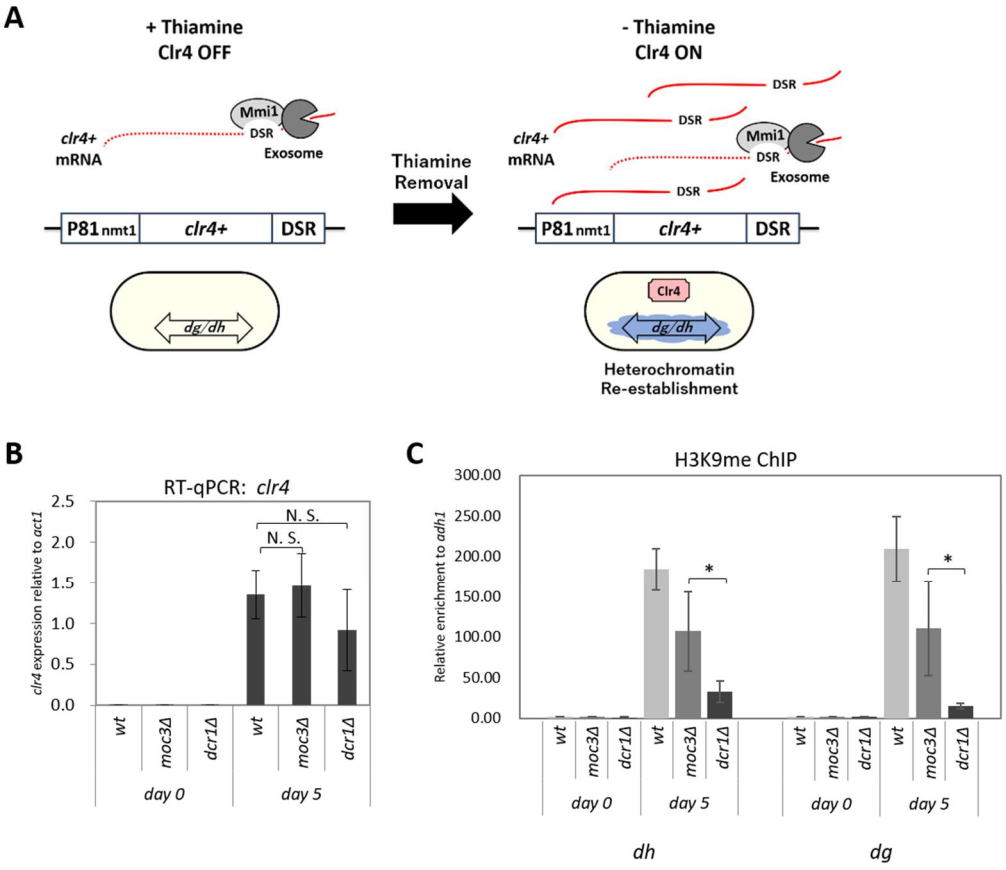

Figure 11. Moc3 is involved in de novo formation of heterochromatin.

(A) Schematic diagram of the Clr4-ON/OFF experiment. The thiamine-repressible *clr4*+ gene is fused with a determinant of selective removal sequence (DSR) recognized by an RNA binding protein Mmi1, which selectively degrades *clr4*+ mRNA. In a medium containing thiamine, slightly leaked *clr4*+ mRNA is completely degraded by Mmi1-associated exosome, and *clr4*+ expression is turned off, whereas in a medium without thiamine, *clr4*+ expression is induced and turned on.

(B) RT-qPCR of *clr4*+ transcripts in indicated strains. Expression levels were normalized by *act1*+. Error

bars indicate the standard deviations from three independent experiments (n=3). P-value was determined using a two-sided Student's t-test: N.S. not significant.

(C) ChIP assay of H3K9me at *dg* and *dh* repeats relative to *adh1+* control locus in indicated strains. Error bars indicate the standard deviations from three independent experiments (n=3). P-value was determined using a two-sided Student's t-test: *p<0.05.

3-6. Moc3 prolongs the chronological life span of cells in the stationary phase by suppressing heterochromatin over-accumulation in rDNA repeats.

rDNA of *S. pombe* contains 100-150 repeat sequences on both ends of chromosome III, and a single repeat consists of *18S*, *5.8S*, and *28S* rRNA genes transcribed by RNA Polymerase I (PolI) [54]. In mitotic dividing cells, RNAi and CCR4-NOT regulate heterochromatin assembly and suppress homologous recombination by releasing RNA Polymerase II (PolII) from rDNA repeats, thus maintaining rDNA integrity [55, 56, 57]. When cells are exposed to nitrogen starvation, cells enter a non-dividing G0 phase called quiescence, and cells restart the cell cycle when cells return to a rich medium. In quiescent cells, RNAi promotes the release of PolI from rDNA repeats, preventing DNA damage and subsequent cell death due to heterochromatin over-accumulation [56]. A recent study also revealed that when cells are exposed to glucose starvation, transcription factor, Atf1 and histone acetyltransferase Gcn5, which promote histone turnover to inhibit the accumulation of methylated H3K9 at rDNA repeats, are dissociated from rDNA repeats. This facilitates the recruitment of FACT, which prevents histone turnover and promotes heterochromatin assembly [58]. Heterochromatin formation at rDNA repeats in response to glucose starvation saves cellular energy and is important for cell survival.

In Pombase, cells lacking heterochromatin regulators such as *ago1+*, *atf1+*, *cid12+*, *clr3+*, *clr4+*, *dcr1+*, *epe1+*, *pob3+*, *rdp1+*, *rik1+*, *sir2+*, *swi6+*, and *tas3+* have been reported to indicate a loss of viability phenotype during G0 and stationary phase. Since loss of viability phenotypes have also been reported in *moc3Δ* cells at G0 and stationary phase, we speculate that Moc3 is involved in facultative heterochromatin at rDNA repeats. To investigate this possibility, we measured chronological life span (CLS), defined as the period of cell survival after the cell enters the stationary phase of the non-dividing state. In wild-type cells, the CLS was 10 days, whereas in *moc3Δ* cells, the CLS was 4 days, resulting in a shorter lifespan (Figure 12A).

In G0 quiescent cells, RNAi mutants were defective in the release of PolI from rDNA repeats, leading to over-accumulation of H3K9me and DNA damage represented by the accumulation of γH2AX a marker of DSB, resulting in the loss of viability of cells [56]. Therefore, we examined the level of H3K9me in rDNA repeats by the ChIP assay. In *moc3Δ* cells, H3K9me levels were increased both in the *18S* and *28S* rDNA repeats compared to wild-type cells (Figure 12B). Note that the ChIP samples were cultured under normal growth conditions, and more pronounced results may be obtained with stationary phase cells. These results suggest that deletion of *moc3+* results in the increase of H3K9me level in rDNA repeats and over-accumulation of heterochromatin leads to cell death representing the shortening of the CLS.

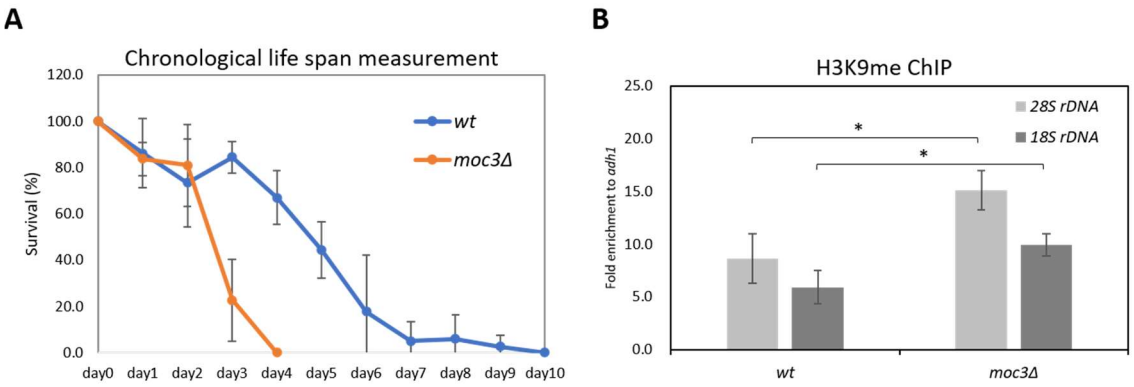

Figure 12. Moc3 is involved in the regulation of facultative heterochromatin in rDNA repeats.

(A) Chronological life span (CLS) measurement. Day 0 indicates the cell enters the stationary phase of the non-dividing state (100% survival, no more division). Colonies were counted on each day until the number of colonies was below 1% (number of colonies = number of viable cells).

(B) ChIP assay of H3K9me at *28S rDNA* and *18S rDNA* repeats relative to *adh1+* control locus in indicated strains. Error bars indicate the standard deviations from three independent experiments (n=3). P-value was determined using a two-sided Student's t-test: *p<0.05.

4. Discussion

How heterochromatic ncRNAs are transcribed from pericentromeric repeats by RNA polymerase II has been unclear. Based on the results of this study, we identified the DNA-binding transcription factor Moc3 as one of the transcriptional activators that activate strand-specific transcription of pericentromeric heterochromatin. We also demonstrated a novel role of the zinc finger protein Moc3 in RNAi-dependent heterochromatin establishment at *dg/dh*. Moc3 localizes to pericentromeric *dh* repeats via its zinc finger domain-dependent manner and specifically activates *dh-Fw* transcription when heterochromatin is compromised. Although Moc3 is not essential for heterochromatin maintenance, its absence significantly reduces the efficient re-establishment of heterochromatin. The process of establishing heterochromatin from scratch is complex, with several transition state barriers due to the presence of numerous silencing factors. Moc3 is expected to be one of the factors supporting this process. Our findings indicate that Moc3 acts as a transcription factor that activates *dh-Fw* transcription, contributing to the RNAi-dependent establishment of pericentromeric heterochromatin (Figure 13).

4-1. Regulation of *dh*-transcription during the establishment and maintenance of heterochromatin.

In *S. pombe*, *dg/dh* repeats in pericentromeric heterochromatin are transcribed bi-directionally from the major promoters within *dg/dh* by RNA polII [18, 50]. During the initial step of the heterochromatin establishment, *dg/dh* transcripts are degraded by exosomes to generate priRNAs. Ago1 then binds to the priRNAs and targets the nascent transcripts transcribed from *dg/dh* to promote RNAi-dependent heterochromatin formation [38]. Targeting of Ago1 facilitates the recruitment of other heterochromatin assembly factors, and local enrichment of these factors at the nucleation site is required for the initiation of heterochromatin formation [60]. Our results indicate that Moc3 provides the substrate of priRNA and/or the target of the Ago1-priRNA complex by stimulating *dh-Fw* transcription during the initial step of the heterochromatin establishment (Figure 13A). Since forward transcripts are more abundant than reverse transcripts in *dg/dh*, Moc3-dependent *dh-Fw* transcription might play a major role in the heterochromatin establishment. Once heterochromatin is established, heterochromatin excludes Moc3 from *dg/dh* and represses transcription by TGS (Figure 13 B). Then, the JmjC-domain protein Epe1 is recruited to heterochromatin in a Swi6-dependent manner and activates transcription from multiple transcription start sites within the *dg/dh* to promote RNAi-dependent heterochromatin

formation [37]. In the absence of Moc3, Epe1 supplies enough amount of *dg/dh*, supporting efficient siRNA production and heterochromatin maintenance. In contrast, in the initial stage of the heterochromatin establishment, Epe1 cannot activate *dg/dh* transcription due to the absence of Swi6 (Figure 13A).

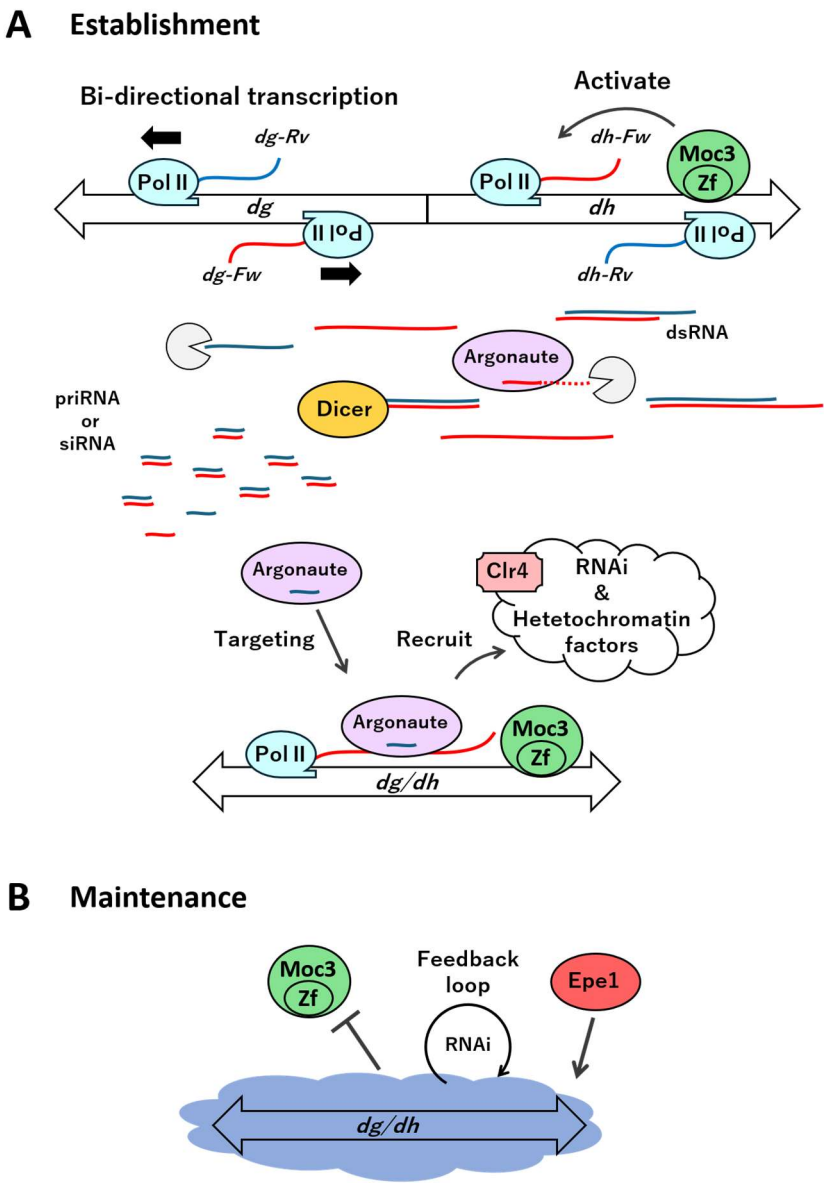

Figure 13. Moc3 acts as a transcription factor to activate *dh-Fw* transcription and contributes to the RNAi-dependent establishment of pericentromeric heterochromatin.

Schematic diagram of models for the Moc3-dependent regulation of *dh*-transcription during establishment and maintenance of pericentromeric heterochromatin. For details, see text.

4-2. Moc3 affects the establishment of heterochromatin not only in *dh* but also in *dg*.

Previous studies have shown that *dg* and *dh* sequences have independent activity in the establishment of heterochromatin [9, 19, 25]. However, our results indicated that even though Moc3 is less associated with *dg* and is not required for transcription from *dg*, the establishment of heterochromatin in *dg* was also impaired in *moc3Δ* cells in both the Clr4 add-back and Clr4 ON/OFF experiments (Figure 7A, 9B, 10E, 11C). Furthermore, as with *dh* siRNA, the amount of *dg* siRNA was reduced by half in *moc3Δ clr3Δ* cells compared to *clr3Δ* cells (Figure 7E). These results suggest that Moc3 is responsible for the establishment of heterochromatin in *dg* as well as *dh*. The amount of forward transcripts is more than 10-fold higher than reverse transcripts, suggesting that the reduction of *dh-Fw* transcripts in *moc3Δ* cells contributes to the primary effect on heterochromatin establishment (Figure 7A, 7B, 7C).

Note that in *moc3Δ* cells, *dh-Fw* transcription does not completely disappear, and a trace amount of weak transcription is still active (Figure 5D). This suggests that weak, albeit inefficient, *dh-Fw* transcription may be sufficient to re-establish heterochromatin. Indeed, in the Clr4 add-back experiment, heterochromatin was re-established in some cells even in the absence of Moc3 (*moc3*Δ *clr4+ (re) red* cells in Figure 10). A recent study revealed that the heterochromatic lncRNA *SPNCRNA.230* and its homologous sequences located in the *dh* repeats of centromere1, centromere2, and *cenH* at the mat locus trigger de novo establishment of heterochromatin [61]. *SPNCRNA.230* transcripts are recognized by the RNA quality control complex MTREC/NURS, which recruits Clr4 to chromatin. Once heterochromatin is established, the sRNA generation becomes more efficient, facilitating Clr4 recruitment. This supports the above possibility.

It is known that a trimethylguanosine synthase Tgs1 also contributes to the heterochromatin establishment by forming trimethylguanosine caps of small nuclear RNA and *dg* transcripts. This modification by Tgs1 contributes to the stable formation of spliceosome on transcripts and/or the retention of *dg* transcripts on chromatin and assists the recruitment of RNAi factors that are important for heterochromatin establishment [62]. Like Moc3, Tgs1 also poorly contributes to heterochromatin maintenance but is required for heterochromatin establishment. Under normal growth conditions, heterochromatin is stable, and there is no need for the establishment system to function in this situation. However, in response to environmental signals such as heat shock, DNA damage, and nutrition starvation, heterochromatin is disrupted, and the Moc3- and Tgs1-regulated establishment systems may contribute to the rapid recovery of heterochromatin.

4-3. Moc3 is involved in facultative heterochromatin.

A previous study has reported that *moc3Δ* cells exhibit multiple phenotypes, including low mating efficiency, sensitivity to $CaCl_2$, and sensitivity to DNA damaging agents such as methyl methanesulfonate (MMS) and UV, indicating that Moc3 is involved in cell survival against stress, maintenance of DNA integrity and DNA damage control [41]. However, it is difficult to explain these phenotypes solely in terms of the compromised establishment of constitutive heterochromatin observed in our experiments. In *S.pombe*, facultative heterochromatin scattered throughout genomes is assembled and disassembled in response to environmental signals such as nutrient conditions, temperature, and DNA damaging agents to regulate gene expression for cell survival [12, 35, 36]. We hypothesized that the multiple phenotypes of *moc3Δ* cells are due to the facultative heterochromatin and measured the viability of cells as they entered the nutrient-deficient stationary phase, which is reduced in RNAi mutants. In our experiments, the deletion of *moc3+* reduced the viability of cells in the stationary phase, as represented by a shortened CLS, and increased H3K9me levels in rDNA repeats even under normal growth conditions (Figure 12). Therefore, it is possible that Moc3 is involved in the regulation of facultative heterochromatin at rDNA repeats in response to environmental signals.

4-4. Functional homologs of Moc3 in other eukaryotes.

Although the detailed mechanisms vary from organism to organism, RNAi-dependent heterochromatin formation is widely conserved in eukaryotes, such as *A. thaliana* and *C. elegance* [63]. The core processes of RNAi-dependent heterochromatin formation are the production of small RNAs and the targeting of sRNA-bound Argonaute to chromatin using sequence complementarity, thereby inducing heterochromatin formation. However, it remains unclear how transcription from heterochromatin is regulated during the establishment and maintenance. Although Moc3 is conserved only in *Schizosaccharomyces japonicus*, it is speculated that functionally homologous factors of Moc3 may exist in other species and activate initial transcription from heterochromatin, and promote heterochromatin establishment. A recent study reported that the zinc finger protein ZNF512 and its paralogue ZNF512B specifically localize to pericentromeric regions through their zinc finger domains and recruit H3K9 methyltransferase SUV39H in mouse embryonic stem cells [64]. ZNF512/ZNF512B can induce de novo establishment of heterochromatin, suggesting that zinc finger proteins are important for the heterochromatin establishment in other species as well in *S. pombe*.

5. Conclusion

We propose a model in which Moc3 acts as a transcription factor that activates *dh-Fw* transcription and contributes to the RNAi-dependent establishment of pericentromeric heterochromatin. Although Moc3 is not essential for heterochromatin maintenance, Moc3 localizes to pericentromeric *dh* repeats via its zinc finger domain-dependent manner and activates *dh* forward transcription when heterochromatin structure is compromised. Furthermore, the absence of Moc3 leads to a significant reduction of siRNA and inefficient re-establishment of heterochromatin. Therefore, Moc3 plays a crucial role in diverse cellular processes by supporting the efficient establishment of constitutive heterochromatin and the regulation of facultative heterochromatin when cells are exposed to environmental stress and heterochromatin is compromised.

6. References

[1] Y. Ogiyama and K. Ishii, "The smooth and stable operation of centromeres," *Genes Genet. Syst*, vol. 87, pp. 63–73, 2012.

[2] B. Fierz and M. G. Poirier, "Biophysics of Chromatin Dynamics," 2019, doi: 10.1146/annurev-biophys-070317.

[3] P. B. Talbert and S. Henikoff, "Histone variants at a glance," 2021, doi: 10.1242/jcs.244749.

[4] A. Stirpe and P. Heun, "The ins and outs of CENP-A: Chromatin dynamics of the centromere-specific histone," *Semin Cell Dev Biol*, vol. 135, pp. 24–34, 2023, doi: 10.1016/j.semcdb.2022.04.003.

[5] O. Morrison and J. Thakur, "Molecular complexes at euchromatin, heterochromatin and centromeric chromatin," *Int J Mol Sci*, vol. 22, no. 13, Jul. 2021, doi: 10.3390/ijms22136922.

[6] K. Tsukii, S. Takahata, and Y. Murakami, "Histone variant H2A.Z plays multiple roles in the maintenance of heterochromatin integrity," *Genes to Cells*, vol. 27, no. 2, pp. 93–112, Feb. 2022, doi: 10.1111/GTC.12911.

[7] H. Zhang, W. Qin, H. Romero, H. Leonhardt, M. C. Cardoso, and M. Cristina, "Heterochromatin organization and phase separation," *Nucleus*, 2023, doi: 10.1080/19491034.2022.2159142.

[8] M. Zofall, S. Yamanaka, F. E. Reyes-Turcu, K. Zhang, C. Rubin, and S. I. S. Grewal, "RNA Elimination Machinery Targeting Meiotic mRNAs Promotes Facultative Heterochromatin Formation," *Science*, vol. 335, no. 6064, p. 96, Jan. 2012, doi: 10.1126/SCIENCE.1211651.

[9] S. Yamanaka *et al.*, "RNAi triggered by specialized machinery silences developmental genes and retrotransposons," *Nature*, vol. 493, no. 7433, pp. 557–560, Jan. 2013, doi: 10.1038/NATURE11716.

[10] P. S. Gallagher *et al.*, "Iron homeostasis regulates facultative heterochromatin assembly in adaptive genome control," *Nat Struct Mol Biol*, vol. 25, no. 5, pp. 372–383, May 2018, doi: 10.1038/S41594-018-0056-2.

[11] Songtao Jia, Ken-ichi Noma, and Shiv I S Grewal, "RNAi-independent heterochromatin nucleation by the stress-activated ATF/CREB family proteins," *Science (1979)*, vol. 304, no. 5679, pp. 1971–1976, 2004, Accessed: Nov. 13, 2023. [Online]. Available: https://www.science.org/doi/10.1126/science.1099035?url_ver=Z39.88-

2003&rfr_id=ori:rid:crossref.org&rfr_dat=cr_pub%20%200pubmed

[12] H. Soo Kim, E. Shik Choi, J. A. Shin, Y. Kyu Jang, and S. Dai Park, "Regulation of Swi6/HP1-dependent Heterochromatin Assembly by Cooperation of Components of the Mitogen-activated Protein Kinase Pathway and a Histone Deacetylase Clr6*," *J Biol Chem*, vol. 279, no. 41, pp. 42850–42859, 2004, doi: 10.1074/jbc.M407259200.

[13] L. Aguilar-Arnal, F. X. Marsellach, and F. Azorín, "The fission yeast homologue of CENP-B, Abp1, regulates directionality of mating-type switching," *EMBO Journal*, vol. 27, no. 7, pp. 1029–1038, Apr. 2008, doi: 10.1038/EMBOJ.2008.53.

[14] T. A. Volpe, C. Kidner, I. M. Hall, G. Teng, S. I. S. Grewal, and R. A. Martienssen, "Regulation of heterochromatic silencing and histone H3 lysine-9 methylation by RNAi," *Science (1979)*, vol. 297, no. 5588, pp. 1833–1837, Sep. 2002, doi: 10.1126/SCIENCE.1074973/SUPPL_FILE/VOLPESOM.PDF.

[15] I. M. Hall, G. D. Shankaranarayana, K. ichi Noma, N. Ayoub, A. Cohen, and S. I. S. Grewal, "Establishment and Maintenance of a Heterochromatin Domain," *Science (1979)*, vol. 297, no. 5590, pp. 2232–2237, Sep. 2002, doi: 10.1126/SCIENCE.1076466.

[16] M. Bühler, W. Haas, S. P. Gygi, and D. Moazed, "RNAi-Dependent and -Independent RNA Turnover Mechanisms Contribute to Heterochromatic Gene Silencing," *Cell*, vol. 129, no. 4, pp. 707–721, May 2007, doi: 10.1016/j.cell.2007.03.038.

[17] F. E. Reyes-Turcu, K. Zhang, M. Zofall, E. Chen, and S. I. S. Grewal, "Defects in RNA quality control factors reveal RNAi-independent nucleation of heterochromatin," *Nature Structural & Molecular Biology 2011 18:10*, vol. 18, no. 10, pp. 1132–1138, Sep. 2011, doi: 10.1038/nsmb.2122.

[18] S. Tashiro, T. Asano, J. Kanoh, and F. Ishikawa, "Transcription-induced chromatin association of RNA surveillance factors mediates facultative heterochromatin formation in fission yeast," *Genes to Cells*, vol. 18, no. 4, pp. 327–339, 2013, doi: 10.1111/gtc.12038.

[19] N. N. Lee *et al.*, "Mtr4-like Protein Coordinates Nuclear RNA Processing for Heterochromatin Assembly and for Telomere Maintenance," *Cell*, vol. 155, no. 5, pp. 1061–1074, 2013, doi: 10.1016/j.cell.2013.10.027.

[20] Y. Chikashige *et al.*, "Composite motifs and repeat symmetry in S. pombe centromeres: Direct analysis by integration of NotI restriction sites," *Cell*, vol. 57, no. 5, pp. 739–751, Jun. 1989, doi: 10.1016/0092-8674(89)90789-7.

[21] H. Kato, D. B. Goto, R. A. Martienssen, T. Urano, K. Furukawa, and Y.

Murakami, "Molecular Biology: RNA polymerase II is required for RNAi-dependent heterochromatin assembly," *Science (1979)*, vol. 309, no. 5733, pp. 467–469, Jul. 2005, doi: 10.1126/SCIENCE.1114955/SUPPL_FILE/KATO.SOM.PDF.

[22] I. Djupedal *et al.*, "RNA Pol II subunit Rpb7 promotes centromeric transcription and RNAi-directed chromatin silencing," *Genes Dev*, vol. 19, no. 19, pp. 2301–2306, Oct. 2005, doi: 10.1101/GAD.344205.

[23] E. S. Chen, K. Zhang, E. Nicolas, H. P. Cam, M. Zofall, and S. I. S. Grewal, "Cell cycle control of centromeric repeat transcription and heterochromatin assembly," *Nature 2008 451:7179*, vol. 451, no. 7179, pp. 734–737, Jan. 2008, doi: 10.1038/nature06561.

[24] A. Verdel *et al.*, "RNAi-Mediated Targeting of Heterochromatin by the RITS Complex," *Science (1979)*, vol. 303, no. 5658, pp. 672–676, Jan. 2004, doi: 10.1126/SCIENCE.1093686/SUPPL_FILE/VERDEL.SOM.REV.PDF.

[25] M. R. Motamedi, A. Verdel, S. U. Colmenares, S. A. Gerber, S. P. Gygi, and D. Moazed, "Two RNAi complexes, RITS and RDRC, physically interact and localize to noncoding centromeric RNAs," *Cell*, vol. 119, no. 6, pp. 789–802, Dec. 2004, doi: 10.1016/j.cell.2004.11.034.

[26] T. Sugiyama, H. Cam, A. Verdel, D. Moazed, and S. I. S. Grewal, "RNA-dependent RNA polymerase is an essential component of a self-enforcing loop coupling heterochromatin assembly to siRNA production," *Proc Natl Acad Sci U S A*, vol. 102, no. 1, pp. 152–157, Jan. 2005, doi: 10.1073/PNAS.0407641102/SUPPL_FILE/07641FIG7.PDF.

[27] J. Nakayama, J. C. Rice, B. D. Strahl, C. D. Allis, and S. I. S. Grewal, "Role of histone H3 lysine 9 methylation in epigenetic control of heterochromatin assembly," *Science (1979)*, vol. 292, no. 5514, pp. 110–113, Apr. 2001, doi: 10.1126/SCIENCE.1060118/SUPPL_FILE/1060118S1_THUMB.GIF.

[28] K. Zhang, K. Mosch, W. Fischle, and S. I. S. Grewal, "Roles of the Clr4 methyltransferase complex in nucleation, spreading and maintenance of heterochromatin," *Nature Structural & Molecular Biology 2008 15:4*, vol. 15, no. 4, pp. 381–388, Mar. 2008, doi: 10.1038/nsmb.1406.

[29] A. J. Bannister *et al.*, "Selective recognition of methylated lysine 9 on histone H3 by the HP1 chromo domain," *Nature 2001 410:6824*, vol. 410, no. 6824, pp. 120–124, Mar. 2001, doi: 10.1038/35065138.

[30] M. Sadaie, T. Iida, T. Urano, and J. I. Nakayama, "A chromodomain protein, Chp1, is required for the establishment of heterochromatin in fission yeast,"

EMBO Journal, vol. 23, no. 19, pp. 3825–3835, Oct. 2004, doi: 10.1038/sj.emboj.7600401.

[31] M. Sadaie *et al.*, "Balance between Distinct HP1 Family Proteins Controls Heterochromatin Assembly in Fission Yeast," *Mol Cell Biol*, vol. 28, no. 23, pp. 6973–6988, Dec. 2008, doi: 10.1128/MCB.00791-08.

[32] S. Takahata *et al.*, "The HMG-box module in FACT is critical for suppressing epigenetic variegation of heterochromatin in fission yeast," *Genes Cells*, vol. 29, no. 7, pp. 567–583, Jul. 2024, doi: 10.1111/GTC.13132.

[33] T. Sugiyama *et al.*, "SHREC, an Effector Complex for Heterochromatic Transcriptional Silencing," *Cell*, vol. 128, no. 3, pp. 491–504, Feb. 2007, doi: 10.1016/j.cell.2006.12.035.

[34] G. D. Shankaranarayana, M. R. Motamedi, D. Moazed, and S. I. S. Grewal, "Sir2 regulates histone H3 lysine 9 methylation and heterochromatin assembly in fission yeast," *Current Biology*, vol. 13, no. 14, pp. 1240–1246, Jul. 2003, doi: 10.1016/S0960-9822(03)00489-5.

[35] T. Yamada, W. Fischle, T. Sugiyama, C. D. Allis, and S. I. S. Grewal, "The nucleation and maintenance of heterochromatin by a histone deacetylase in fission yeast," *Mol Cell*, vol. 20, no. 2, pp. 173–185, Oct. 2005, doi: 10.1016/j.molcel.2005.10.002.

[36] M. Zofall and S. I. S. Grewal, "Swi6/HP1 Recruits a JmjC Domain Protein to Facilitate Transcription of Heterochromatic Repeats," *Mol Cell*, vol. 22, pp. 681–692, 9AD, doi: 10.1016/j.molcel.2006.05.010.

[37] T. Asanuma, S. Inagaki, T. Kakutani, H. Aburatani, and Y. Murakami, "Tandemly repeated genes promote RNAi-mediated heterochromatin formation via an antisilencing factor, Epe1, in fission yeast," *Genes Dev*, vol. 36, no. 21–24, pp. 1145–1159, Nov. 2022, doi: 10.1101/GAD.350129.122/-/DC1.

[38] M. Halic and D. Moazed, "Dicer-Independent Primal RNAs Trigger RNAi and Heterochromatin Formation," *Cell*, vol. 140, no. 4, pp. 504–516, Feb. 2010, doi: 10.1016/j.cell.2010.01.019.

[39] M. Marasovic, M. Zocco, and M. Halic, "Argonaute and triman generate dicer-independent prirnas and mature siRNAs to initiate heterochromatin formation," *Mol Cell*, vol. 52, no. 2, pp. 173–183, Oct. 2013, doi: 10.1016/j.molcel.2013.08.046.

[40] Y. Otsubo and M. Yamamoto, "Signaling pathways for fission yeast sexual differentiation at a glance," *J Cell Sci*, vol. 125, no. Pt 12, pp. 2789–2793, Jun. 2012, doi: 10.1242/JCS.094771.

[41] M. M. Goldar, H. T. Jeong, K. Tanaka, H. Matsuda, and M. Kawamukai, "Moc3, a novel Zn finger type protein involved in sexual development, ascus formation, and stress response of Schizosaccharomyces pombe," *Curr Genet*, vol. 48, no. 6, pp. 345–355, Dec. 2005, doi: 10.1007/s00294-005-0028-z.

[42] M. Sorida *et al.*, "Regulation of ectopic heterochromatin-mediated epigenetic diversification by the JmjC family protein Epe1," *PLoS Genet*, vol. 15, no. 6, Jun. 2019, doi: 10.1371/JOURNAL.PGEN.1008129.

[43] E. Oya, H. Kato, Y. Chikashige, C. Tsutsumi, Y. Hiraoka, and Y. Murakami, "Mediator directs co-transcriptional heterochromatin assembly by RNA interference-dependent and -independent pathways," *PLoS Genet*, vol. 9, no. 8, Aug. 2013, doi: 10.1371/JOURNAL.PGEN.1003677.

[44] R. C. Allshire, E. R. Nimmo, K. Ekwall, J. P. Javerzat, and G. Cranston, "Mutations derepressing silent centromeric domains in fission yeast disrupt chromosome segregation," *Genes Dev*, vol. 9, no. 2, pp. 218–233, Jan. 1995, doi: 10.1101/GAD.9.2.218.

[45] O. Niwa, T. Matsumoto, Y. Chikashige, and M. Yanagida, "Characterization of Schizosaccharomyces pombe minichromosome deletion derivatives and a functional allocation of their centromere," *EMBO Journal*, vol. 8, no. 10, pp. 3045–3052, 1989, doi: 10.1002/J.1460-2075.1989.TB08455.X.

[46] S. Suzuki *et al.*, "Histone H3K36 trimethylation is essential for multiple silencing mechanisms in fission yeast," *Nucleic Acids Res*, vol. 44, no. 9, pp. 4147–4162, May 2016, doi: 10.1093/NAR/GKW008.

[47] T. Kajitani *et al.*, "Ser7 of RNAPII-CTD facilitates heterochromatin formation by linking ncRNA to RNAi," *Proc Natl Acad Sci U S A*, vol. 114, no. 52, pp. E11208–E11217, Dec. 2017, doi: 10.1073/PNAS.1714579115.

[48] S. Takahata, T. Asanuma, M. Mori, and Y. Murakami, "Construction and characterization of a zinc-inducible gene expression vector in fission yeast," *Yeast*, vol. 38, no. 4, pp. 251–261, Apr. 2021, doi: 10.1002/YEA.3539.

[49] K. Kawakami, A. Hayashi, J. I. Nakayama, and Y. Murakami, "A novel RNAi protein, Dsh1, assembles RNAi machinery on chromatin to amplify heterochromatic siRNA," *Genes Dev*, vol. 26, no. 16, pp. 1811–1824, Aug. 2012, doi: 10.1101/GAD.190272.112.

[50] D. Holoch and D. Moazed, "Small-RNA loading licenses Argonaute for assembly into a transcriptional silencing complex," *Nat Struct Mol Biol*, vol. 22, no. 4, pp. 328–335, Apr. 2015, doi: 10.1038/NSMB.2979.

[51] K. Ekwall, G. Cranston, and R. C. Allshire, "Fission yeast mutants that alleviate

transcriptional silencing in centromeric flanking repeats and disrupt chromosome segregation," *Genetics*, vol. 153, no. 3, pp. 1153–1169, Nov. 1999, doi: 10.1093/GENETICS/153.3.1153.

[52] K. Maundrell, "Thiamine-repressible expression vectors pREP and pRIP for fission yeast," *Gene*, vol. 123, no. 1, pp. 127–130, Jan. 1993, doi: 10.1016/0378-1119(93)90551-D.

[53] Y. Harigaya *et al.*, "Selective elimination of messenger RNA prevents an incidence of untimely meiosis," *Nature*, vol. 442, no. 7098, pp. 45–50, Jul. 2006, doi: 10.1038/NATURE04881.

[54] H. Hirai and K. Ohta, "Comparative Research: Regulatory Mechanisms of Ribosomal Gene Transcription in Saccharomyces cerevisiae and Schizosaccharomyces pombe," Feb. 01, 2023, *MDPI*. doi: 10.3390/biom13020288.

[55] H. P. Cam, T. Sugiyama, E. S. Chen, X. Chen, P. C. FitzGerald, and S. I. S. Grewal, "Comprehensive analysis of heterochromatin- and RNAi-mediated epigenetic control of the fission yeast genome," *Nat Genet*, vol. 37, no. 8, pp. 809–819, Aug. 2005, doi: 10.1038/NG1602.

[56] B. Roche, B. Arcangioli, and R. A. Martienssen, "RNA interference is essential for cellular quiescence," *Science (1979)*, vol. 354, no. 6313, Nov. 2016, doi: 10.1126/science.aah5651.

[57] T. Sugiyama *et al.*, "Enhancer of Rudimentary Cooperates with Conserved RNA-Processing Factors to Promote Meiotic mRNA Decay and Facultative Heterochromatin Assembly," *Mol Cell*, vol. 61, no. 5, pp. 747–759, Mar. 2016, doi: 10.1016/j.molcel.2016.01.029.

[58] H. Hirai, N. Takemata, M. Tamura, and K. Ohta, "Facultative heterochromatin formation in rDNA is essential for cell survival during nutritional starvation," *Nucleic Acids Res*, vol. 50, no. 7, pp. 3727–3744, Apr. 2022, doi: 10.1093/nar/gkac175.

[59] A. Kloc, M. Zaratiegui, E. Nora, and R. Martienssen, "RNA Interference Guides Histone Modification during the S Phase of Chromosomal Replication," *Current Biology*, vol. 18, no. 7, pp. 490–495, Apr. 2008, doi: 10.1016/j.cub.2008.03.016.

[60] S. I. S. Grewal, "The molecular basis of heterochromatin assembly and epigenetic inheritance," *Mol Cell*, vol. 83, no. 11, pp. 1767–1785, Jun. 2023, doi: 10.1016/J.MOLCEL.2023.04.020.

[61] J. S. Khanduja *et al.*, "RNA quality control factors nucleate Clr4/SUV39H and

trigger constitutive heterochromatin assembly," *Cell*, vol. 187, no. 13, pp. 3262-3283.e23, Jun. 2024, doi: 10.1016/J.CELL.2024.04.042.

[62] H. Yu *et al.*, "Trimethylguanosine synthase 1 (Tgs1) is involved in Swi6/HP1-independent siRNA production and establishment of heterochromatin in fission yeast," *Genes Cells*, vol. 26, no. 4, pp. 203–218, Apr. 2021, doi: 10.1111/GTC.12833.

[63] S. E. Castel and R. A. Martienssen, "RNA interference in the nucleus: roles for small RNAs in transcription, epigenetics and beyond," *Nat Rev Genet*, vol. 14, no. 2, pp. 100–112, Feb. 2013, doi: 10.1038/NRG3355.

7. Acknowledgements

I would like to express my deepest appreciation to my supervisor Professor Yota Murakami for his encouragement, constructive suggestions, and thoughtful guidance.

I would like to express my gratitude to the thesis committee members, Professor Akinori Takaoka, Professor Kazuyasu Sakaguchi, Professor Fumio Motegi, and Professor Ken'ichiro Matsumoto for their valuable suggestions on my PhD work.

I am also particularly grateful to Assistant Professor Shinya Takahata for his valuable advice discussions and technical support. I would like to thank Professor Masayuki Takahashi and Associate Professor Akiko Nakatomi for their helpful guidance and encouragement. I have had the support and encouragement of all the members of the Laboratory of Bioorganic Chemistry.

I would like to express my gratitude to Professor Jun-ichi Nakayama and Professor Robin Allshire for providing the strains and plasmids, and Professor Takeshi Urano, and Professor Hiroshi Kimura for providing the antibodies.

I would like to express my gratitude to the members of the Institute of Biomedical Research at Sapporo Higashi Tokushukai Hospital for their assistance in writing this doctoral thesis.

Finally, special thanks to my family, friends, and colleagues for their continuous support and encouragement.